**Supporting Information**

# Analysis of Unusual Sulfated Constituents and Anti-infective Properties of Two Indonesian Mangroves, *Lumnitzera littorea* and *Lumnitzera racemosa* (Combretaceae)

Jeprianto Manurung [1,2,3,a], Jonas Kappen[3,a], Jan Schnitzler [1,2], Andrej Frolov [3,4], Ludger A. Wessjohann [2,3], Andria Agusta [5], Alexandra N. Muellner-Riehl [1,2,*] and Katrin Franke [3,*]

[1] Department of Molecular Evolution and Plant Systematics & Herbarium (LZ), Institute of Biology, Leipzig University, Germany; jeprianto_m@apps.ipb.ac.id (J.M.); j.schnitzler06@alumni.imperial.ac.uk (J.S.); muellner-riehl@uni-leipzig.de (A.N.M.-R.)
[2] German Centre for Integrative Biodiversity Research (iDiv) Halle-Jena-Leipzig, Leipzig, Germany
[3] Department of Bioorganic Chemistry, Leibniz Institute of Plant Biochemistry (IPB), Halle (Saale), Germany; katrin.franke@ipb-halle.de (K.F.); andrej.frolov@ipb-halle.de (A.F.); jkappen@ipb-halle.de (J.K.); ludger.wessjohann@ipb-halle.de (L.A.W.)
[4] Department of Biochemistry, St. Petersburg State University, St. Petersburg, Russia
[5] Research Center for Chemistry, Indonesian Institute of Sciences (LIPI), Bogor, Indonesia; andr002@lipi.go.id (A.A.)

* Correspondence: muellner-riehl@uni-leipzig.de (phylogeny); katrin.franke@ipb-halle.de (chemistry); Tel.: +49-341-97-38581 (A.N.M.-R.); +49-345-5582-1380 (K.F.)

[a] J.M and J.K. contributed equally to this work.

**Content** **Page**

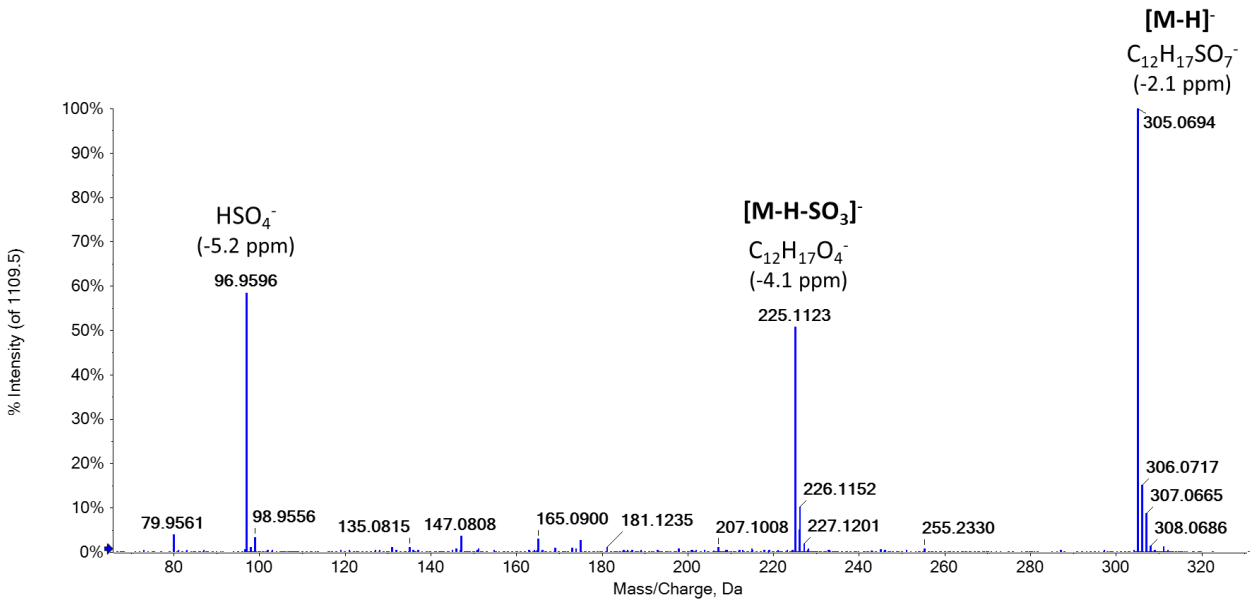


**Figure S1-1.** Tandem mass spectrum of *m/z* 305.0996 at $t_R$ 3.5 min of compound **1**, annotated in methanolic root extract of *Lumnitzera littorea*. The spectrum was acquired with a QqTOF mass spectrometer operated in the negative SWATH mode (*m/z* window 289.0–315.0).

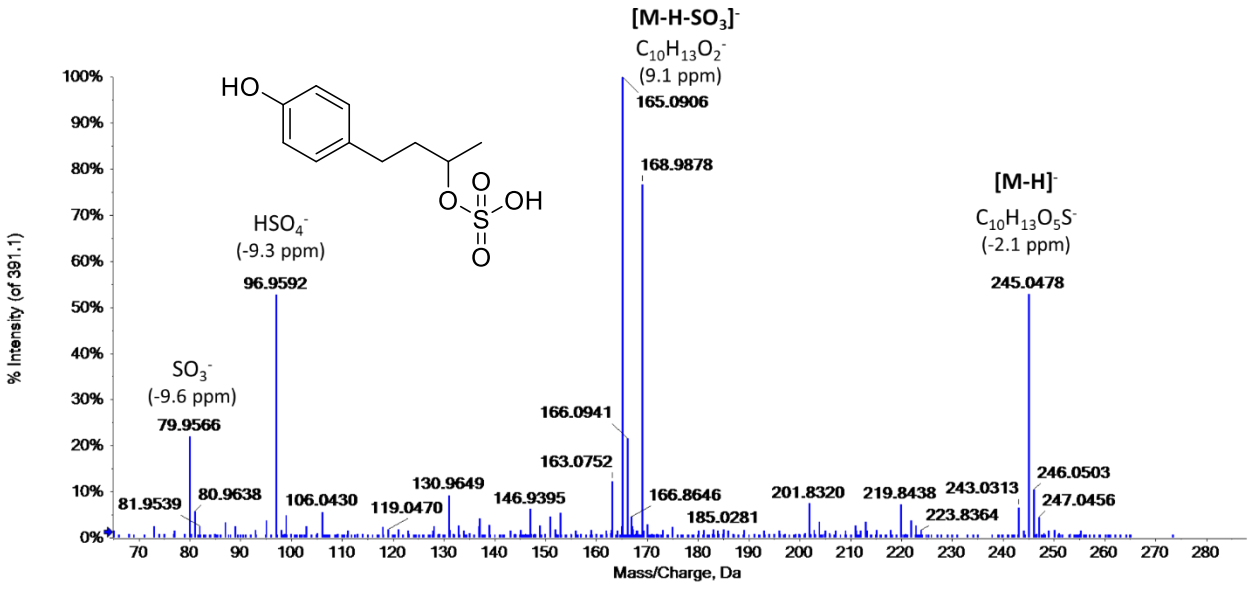


**Figure S1-2.** Tandem mass spectrum of *m/z* 245.0488 at $t_R$ 3.8 min of compound **2**, annotated in methanolic root extracts of *Lumnitzera littorea* and *L. racemosa*. The spectrum was acquired with a QqTOF mass spectrometer operated in the negative SWATH mode (*m/z* window 239.0–265.0).

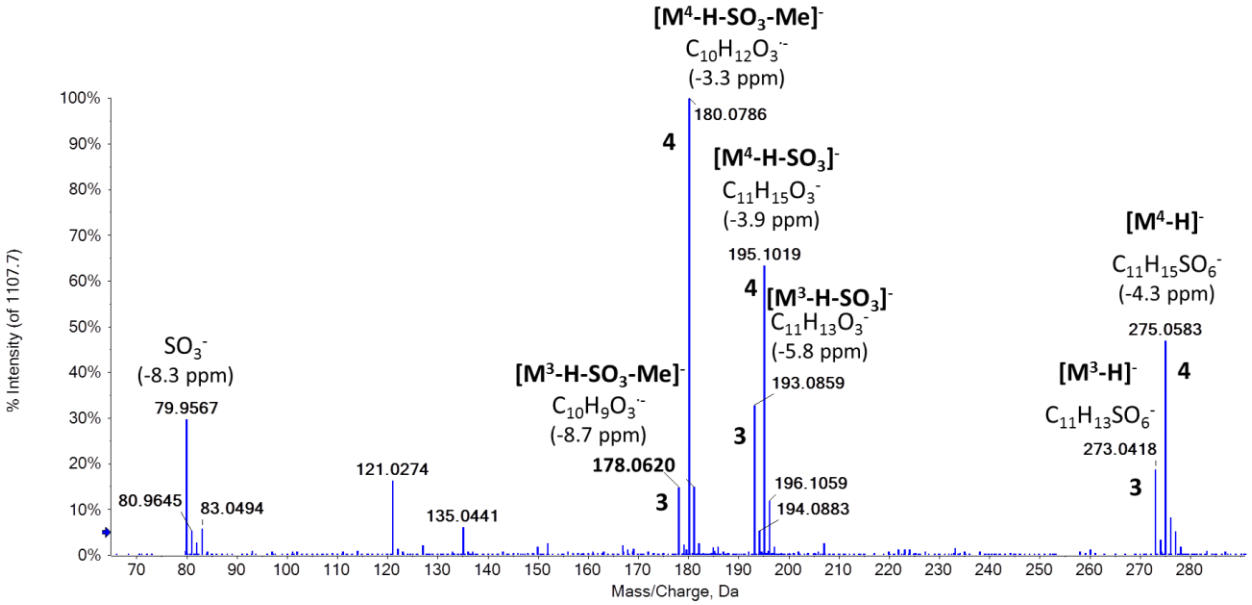


**Figure S1-3.** Tandem mass spectrum of *m/z* 273.0436 and 275.0591 at $t_R$ 3.9 min of overlapping compounds **3** and **4**, respectively, annotated in methanolic root extracts of *Lumnitzera littorea* and *L. racemosa*. The spectrum was acquired with a QqTOF mass spectrometer operated in the negative SWATH mode (*m/z* window 264.0–290.0).

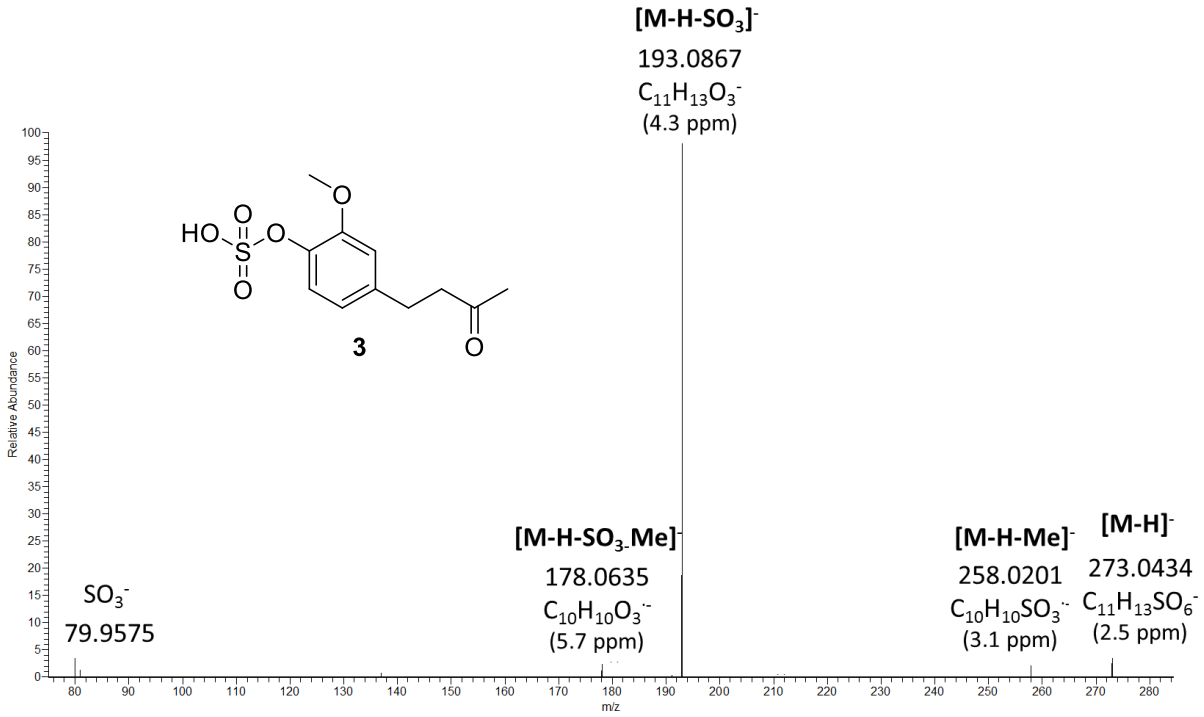


**Figure S1-4.** Tandem mass spectrum of *m/z* 273.0436 at $t_R$ 3.9 min of compound **3**, annotated in methanolic root extracts of *Lumnitzera littorea* and *L. racemosa*. The spectrum was acquired with LIT-Orbitrap-MS in negative ion mode with CID activation (30% relative collision energy).

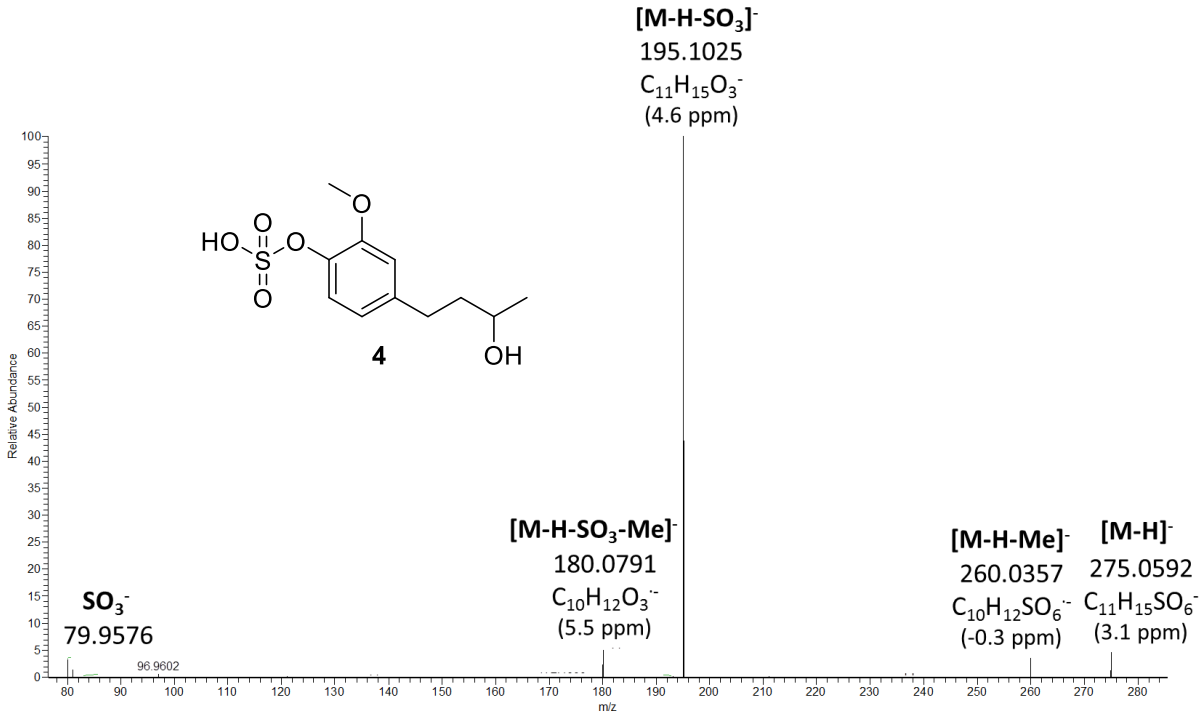


**Figure S1-5.** Tandem mass spectrum of *m/z* 275.0591 at $t_R$ 3.9 min of compound **4**, annotated in methanolic root extracts of *Lumnitzera littorea* and *L. racemosa*. The spectrum was acquired with LIT-Orbitrap-MS in negative ion mode with CID activation (30% relative collision energy).

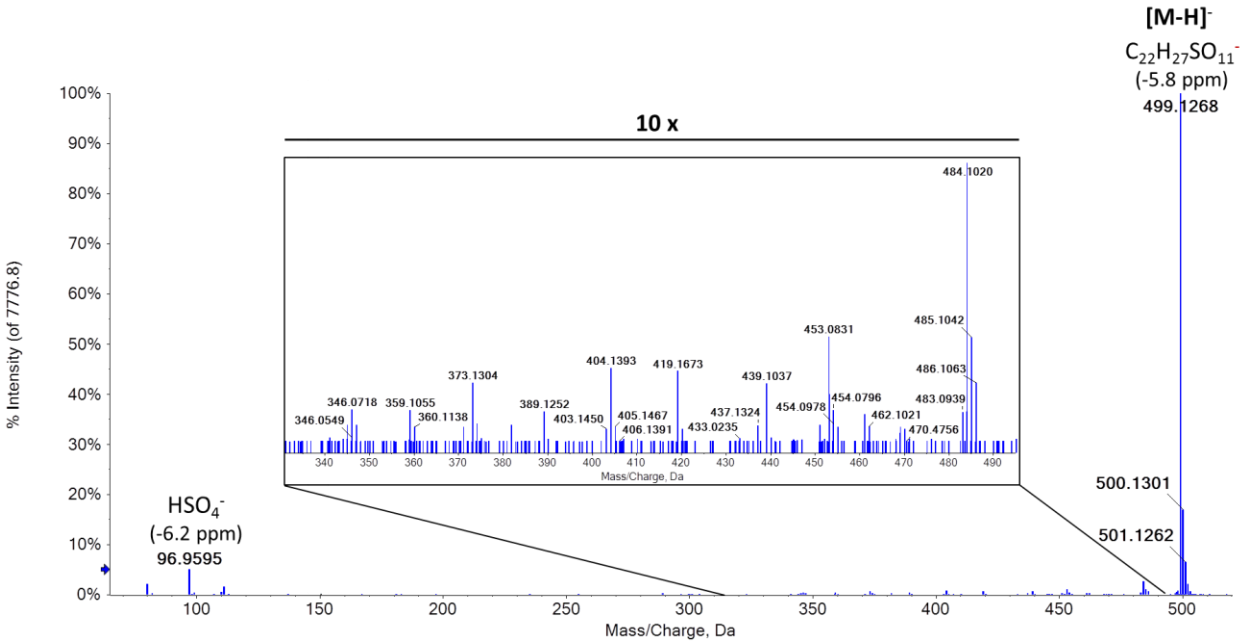


**Figure S1-6.** Tandem mass spectrum of *m/z* 499.1267 at $t_R$ 4.4 min of compound **5**, annotated in methanolic root extracts of *Lumnitzera littorea*. The spectrum was acquired with a QqTOF mass spectrometer operated in the negative SWATH mode (*m/z* window 489.0–515.0).

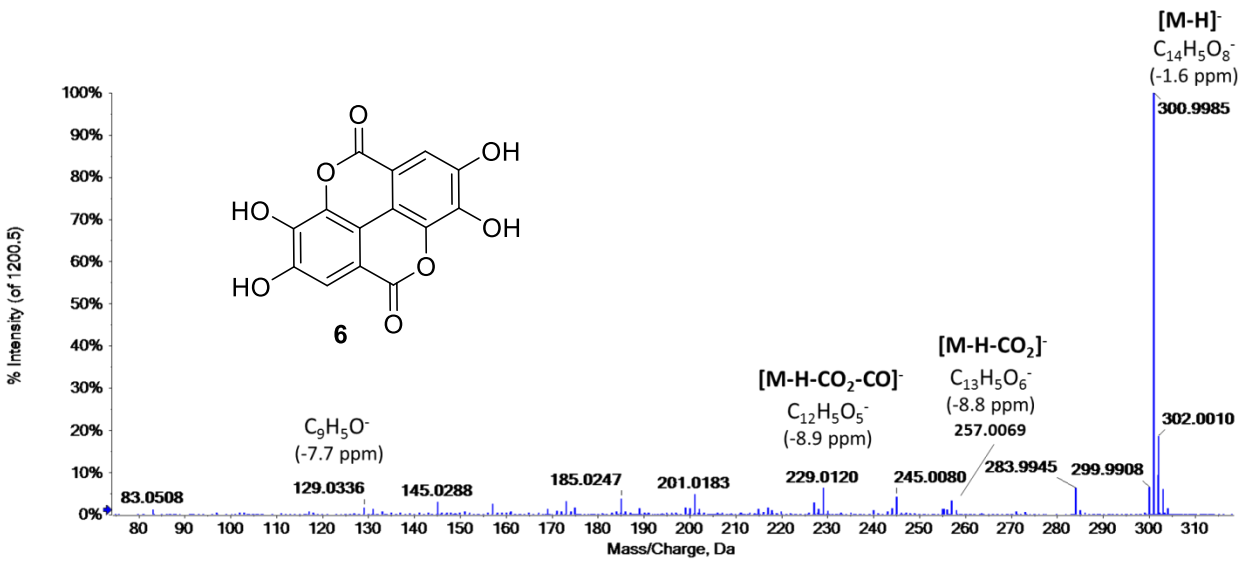


**Figure S1-7.** Tandem mass spectrum of *m/z* 300.9989 at $t_R$ 4.4 min of compound **6**, annotated in methanolic root extracts of *Lumnitzera littorea*. The spectrum was acquired with a QqTOF mass spectrometer operated in the negative SWATH mode (*m/z* window 289.0–315.0).

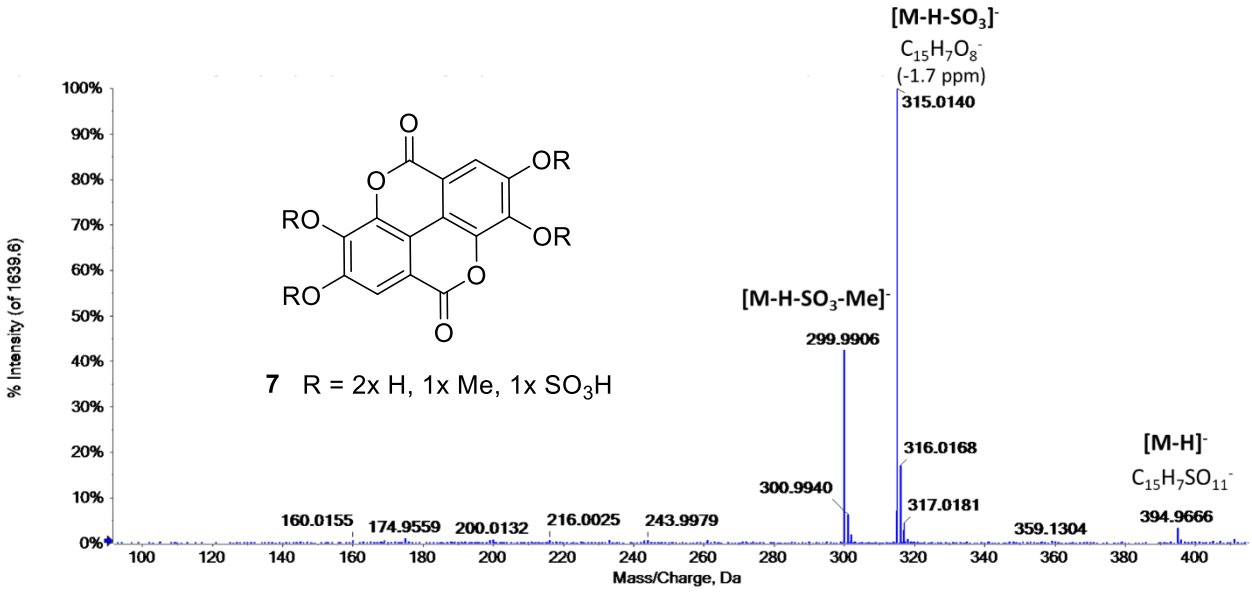


**Figure S1-8.** Tandem mass spectrum of *m/z* 394.9707 at $t_R$ 5.3 min of compound **7**, annotated in methanolic root extracts of *Lumnitzera racemosa*. The spectrum was acquired with a QqTOF mass spectrometer operated in the negative SWATH mode (*m/z* window 389.0–415.0).

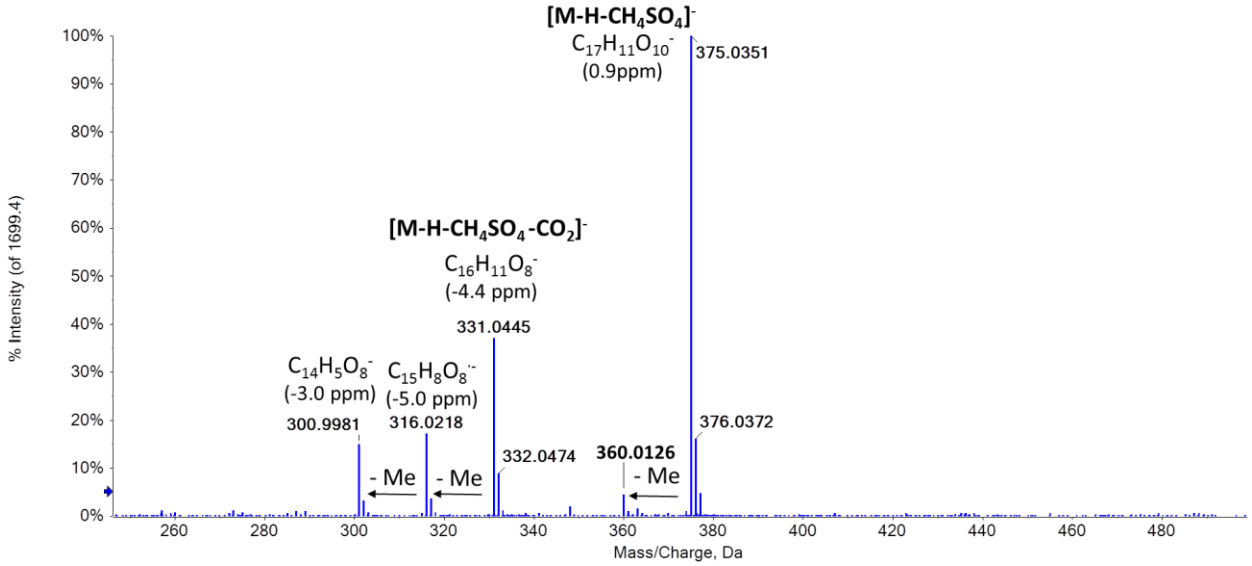


**Figure S1-9.** Tandem mass spectrum of *m/z* 487.0179 at $t_R$ 5.5 min of compound **8**, annotated in the methanolic root extract of *Lumnitzera racemosa*. The spectrum was acquired with a QqTOF mass spectrometer operated in the negative SWATH mode (*m/z* window 464.0–490.0).

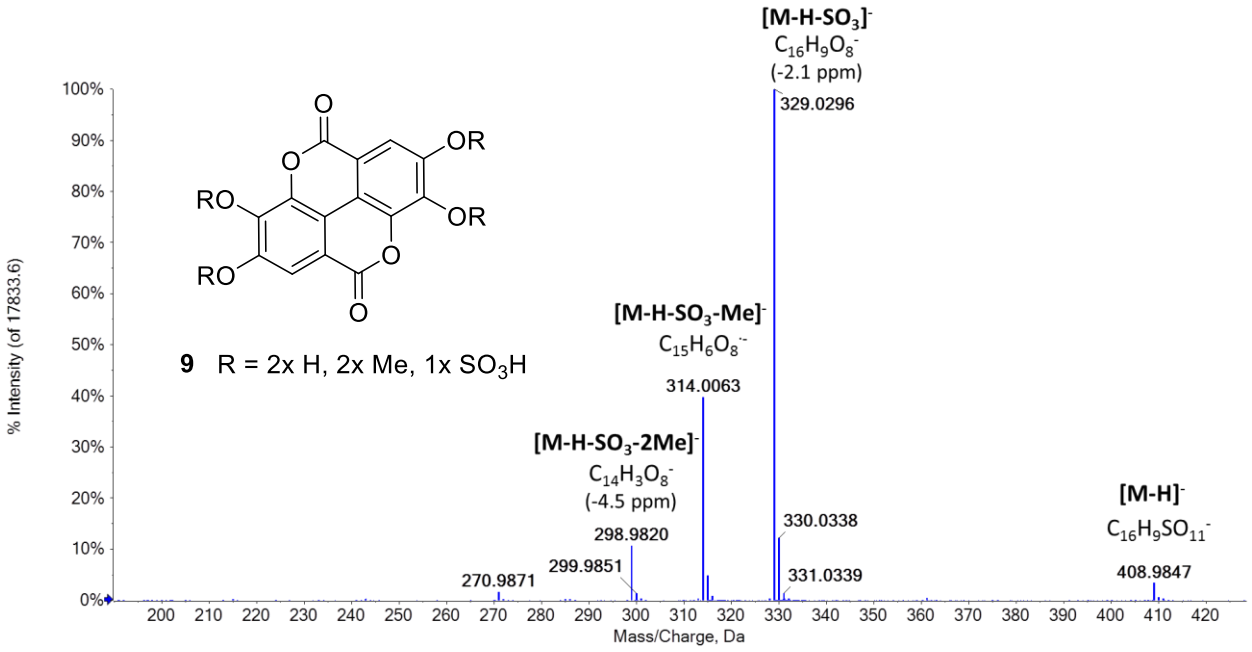


**Figure S1-10.** Tandem mass spectrum of *m/z* 408.9898 at $t_R$ 5.7 min of compound **9**, annotated in methanolic root extracts of *Lumnitzera littorea* and *L. racemosa*. The spectrum was acquired with a QqTOF mass spectrometer operated in the negative SWATH mode (*m/z* window 389.0–415.0).

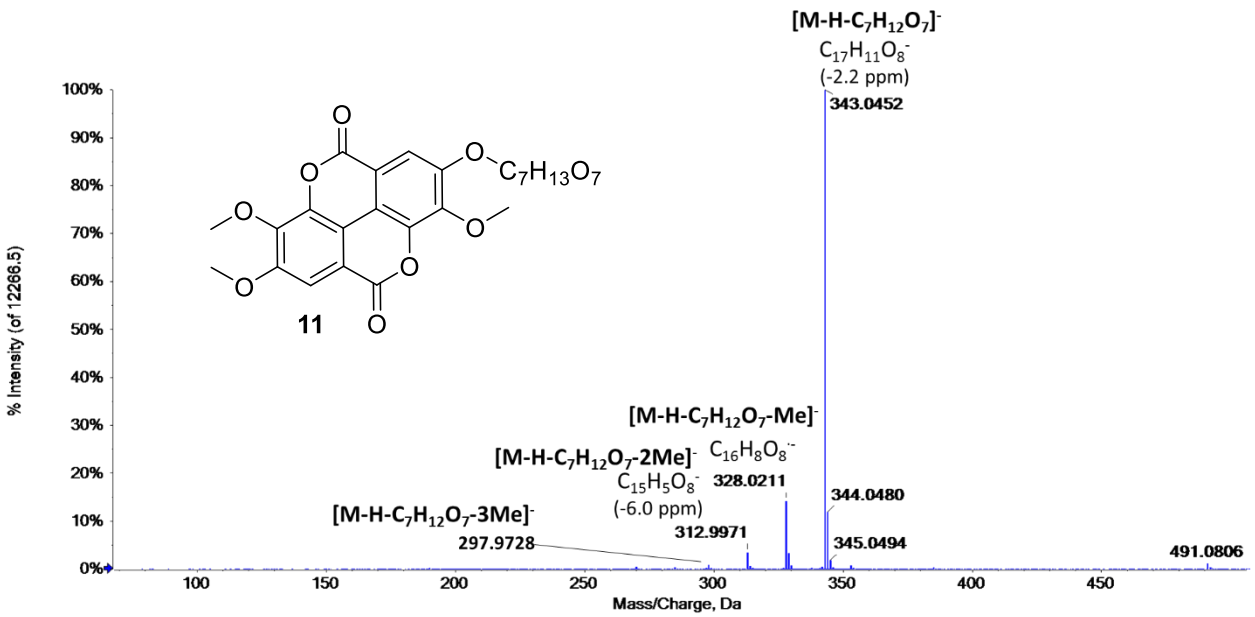


**Figure S1-11.** Tandem mass spectrum of *m/z* 551.1027 at $t_R$ 6.0 min of compound **10**, annotated in methanolic root extracts of *Lumnitzera racemosa*. The spectrum was acquired with a QqTOF mass spectrometer operated in the negative SWATH mode (*m/z* window 539.0–565.0).

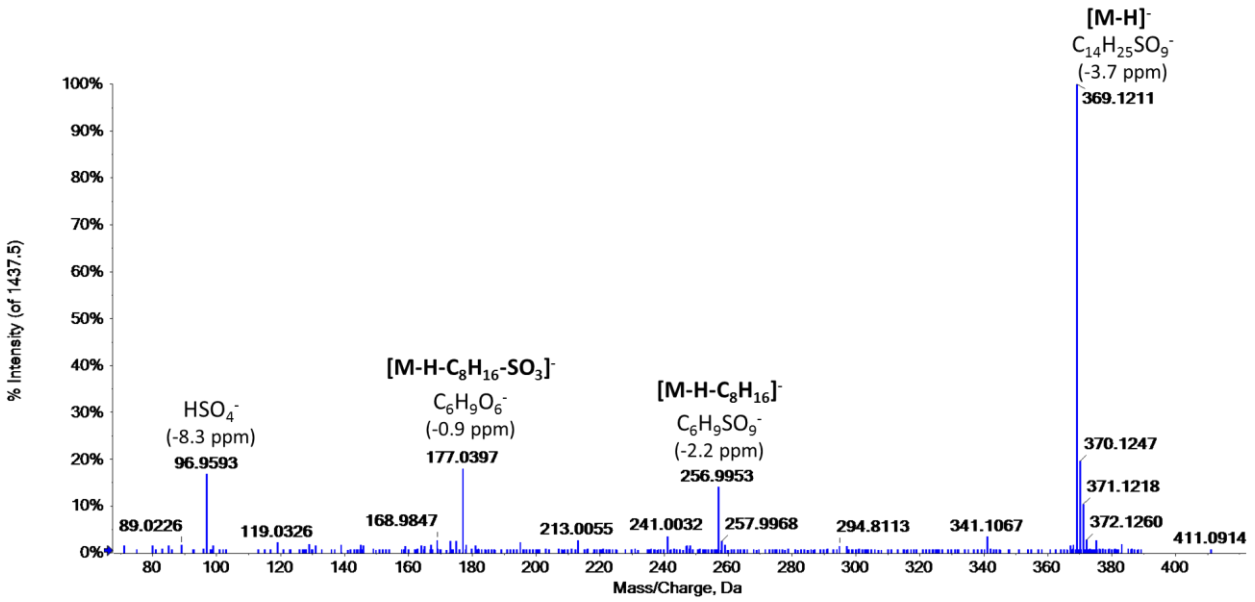


**Figure S1-12.** Tandem mass spectrum of *m/z* 369.1225 at $t_R$ 6.1 min of compound **11**, annotated in methanolic root extracts of *Lumnitzera littorea*. The spectrum was acquired with a QqTOF mass spectrometer operated in the negative SWATH mode (*m/z* window 364.0–390.0).

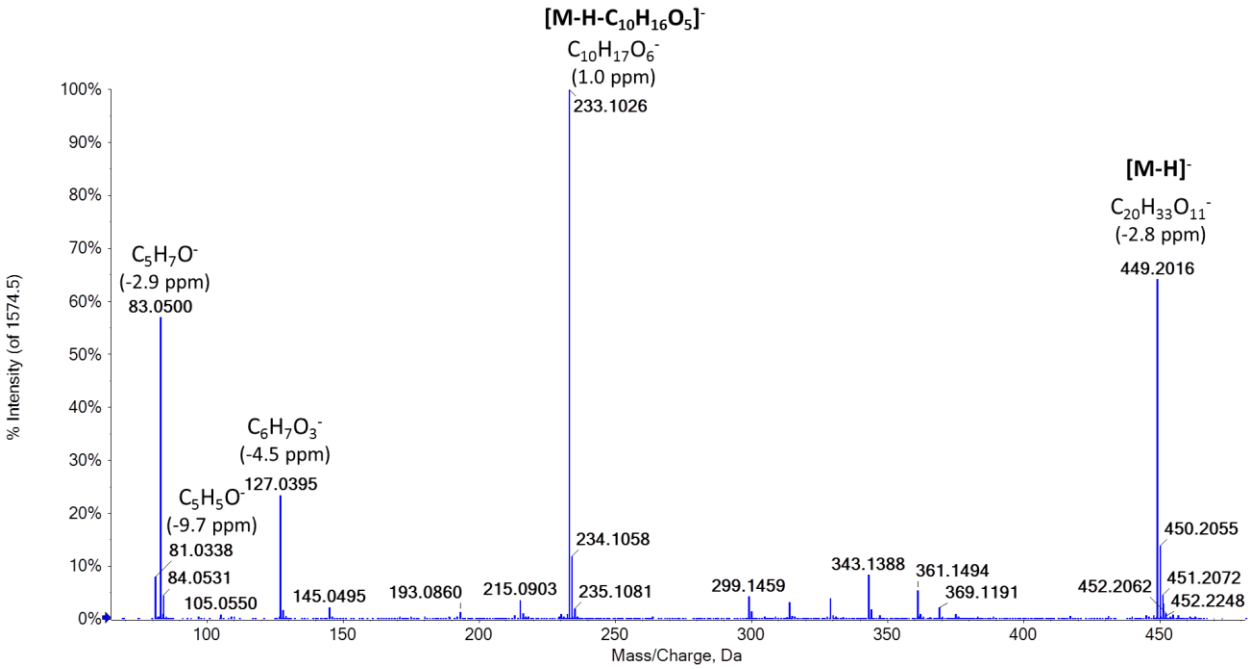


**Figure S1-13.** Tandem mass spectrum of *m/z* 449.2027 at $t_R$ 6.3 min of compound **12**, annotated in methanolic root extracts of *Lumnitzera littorea* and *L. racemosa*. The spectrum was acquired with a QqTOF mass spectrometer operated in the negative SWATH mode (*m/z* window 439.0–465.0).

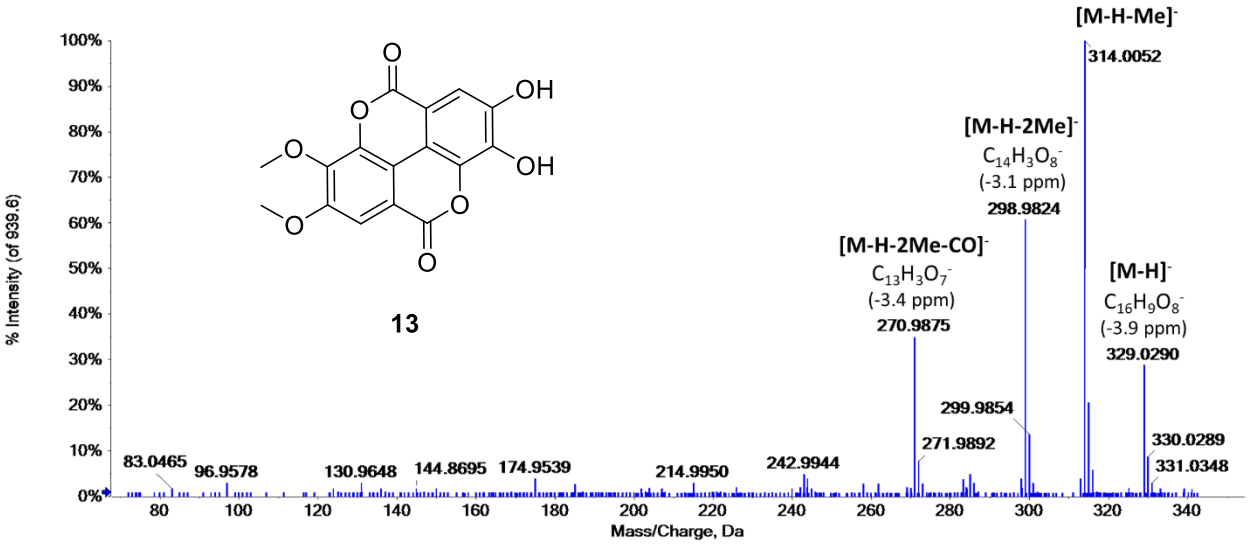


**Figure S1-14.** Tandem mass spectrum of *m/z* 329.0301 at $t_R$ 6.4 min of compound **13**, annotated in methanolic root extracts of *Lumnitzera littorea* and *L. racemosa*. The spectrum was acquired with a QqTOF mass spectrometer operated in the negative SWATH mode (*m/z* window 314.0–340.0).

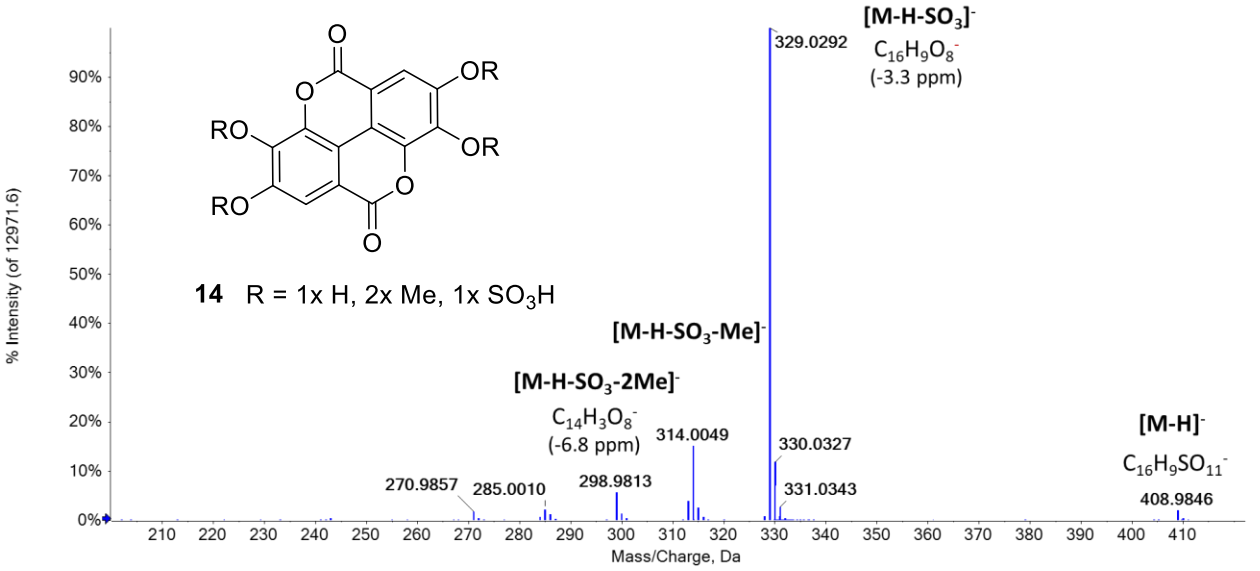


**Figure S1-15.** Tandem mass spectrum of *m/z* 408.9867 at $t_R$ 6.5 min of compound **14**, annotated in methanolic root extracts of *Lumnitzera racemosa*. The spectrum was acquired with a QqTOF mass spectrometer operated in the negative SWATH mode (*m/z* window 389.0–415.0).

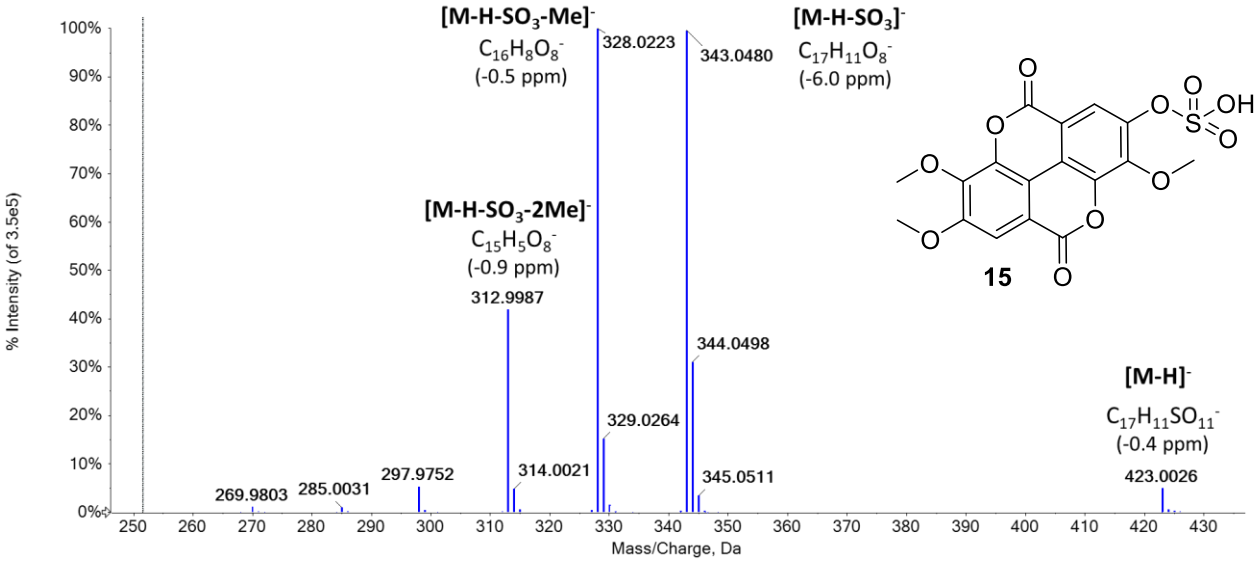


**Figure S1-16.** Tandem mass spectrum of *m/z* 423.0035 at $t_R$ 6.9 min of compound **15**, annotated in methanolic root extracts of *Lumnitzera littorea* and *L. racemosa*. The spectrum was acquired with a QqTOF mass spectrometer operated in the negative SWATH mode (*m/z* window 414.0–440.0).

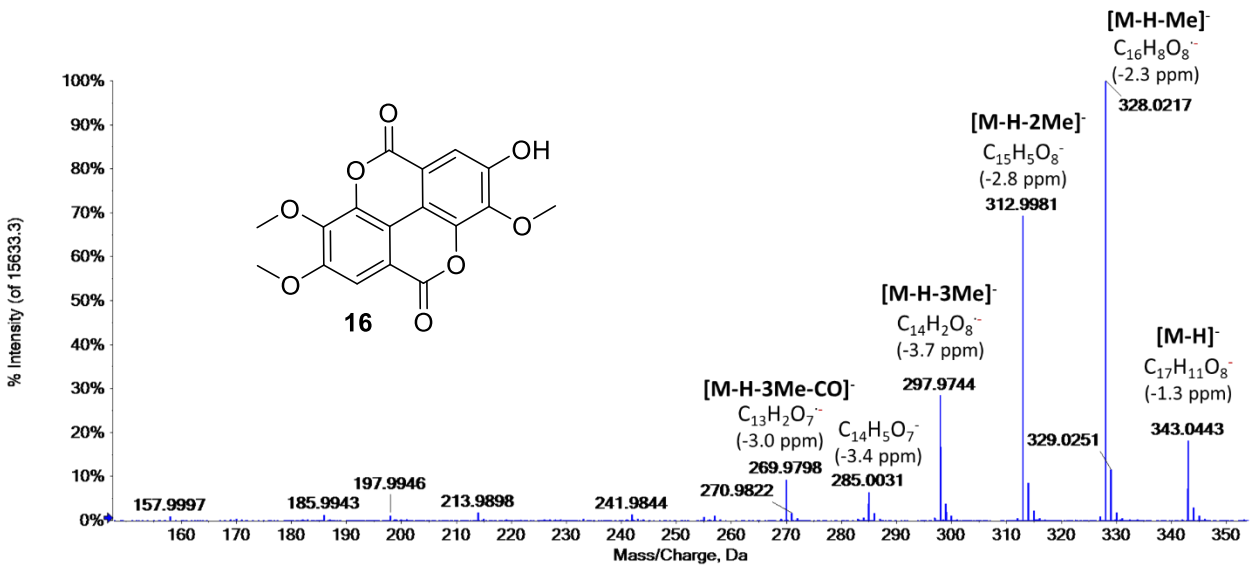


**Figure S1-17.** Tandem mass spectrum of *m/z* 343.0455 at $t_R$ 7.7 min of compound **16**, annotated in methanolic root extracts of *Lumnitzera littorea* and *L. racemosa*. The spectrum was acquired with a QqTOF mass spectrometer operated in the negative SWATH mode (*m/z* window 339.0–365.0).

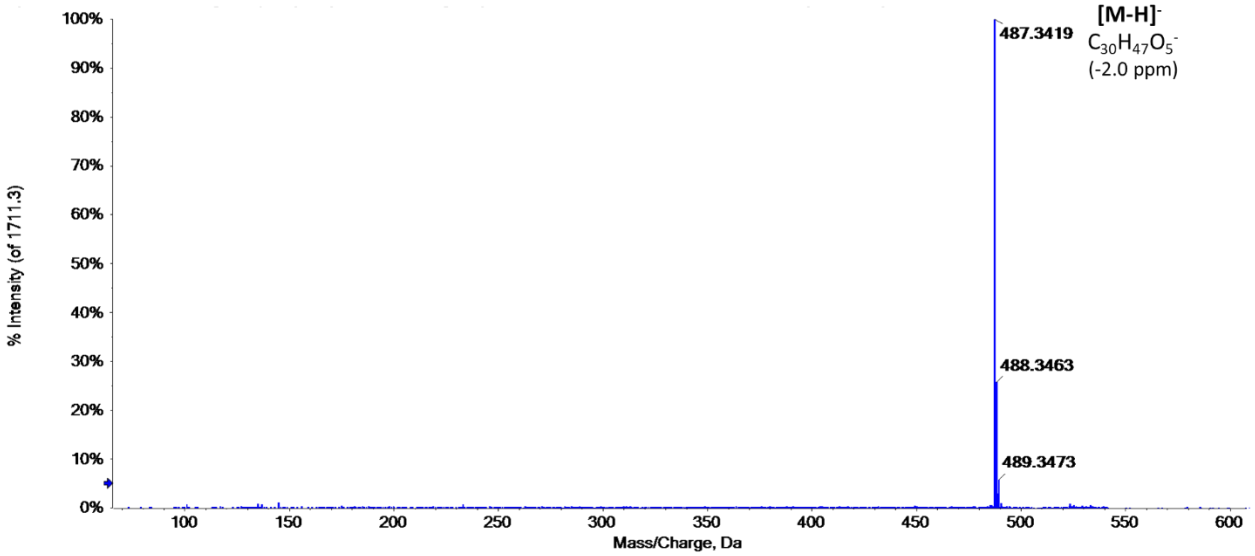


**Figure S1-18.** Tandem mass spectrum of *m/z* 533.3480 at $t_R$ 9.8 min of the formiate adduct of compound **17**, annotated in methanolic root extracts of *Lumnitzera littorea* and *L. racemosa*. The spectrum was acquired with a QqTOF mass spectrometer operated in the negative SWATH mode (*m/z* window 514.0–540.0).

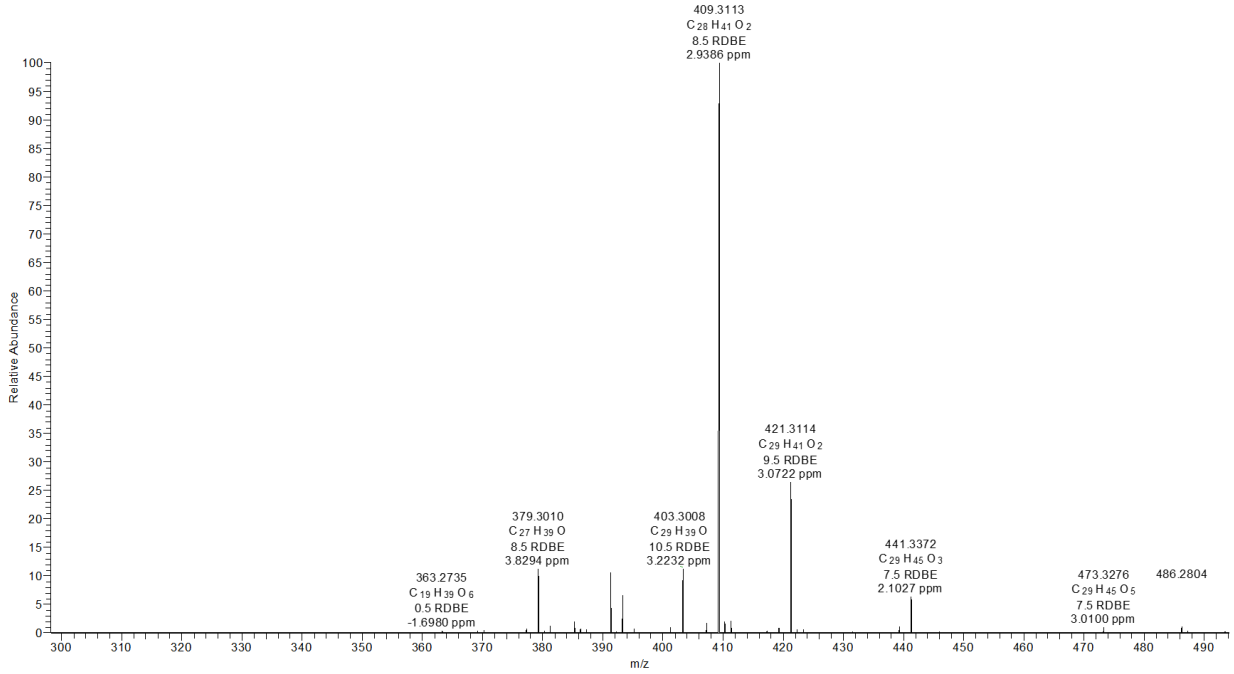


**Figure S1-19.** Tandem mass spectrum of *m/z* 487.3425 at $t_R$ 9.8 min of compound **17**, annotated in methanolic root extracts of *Lumnitzera littorea* and *L. racemosa*. The spectrum was acquired with LIT-Orbitrap-MS in negative ion mode with CID activation (35% relative collision energy).

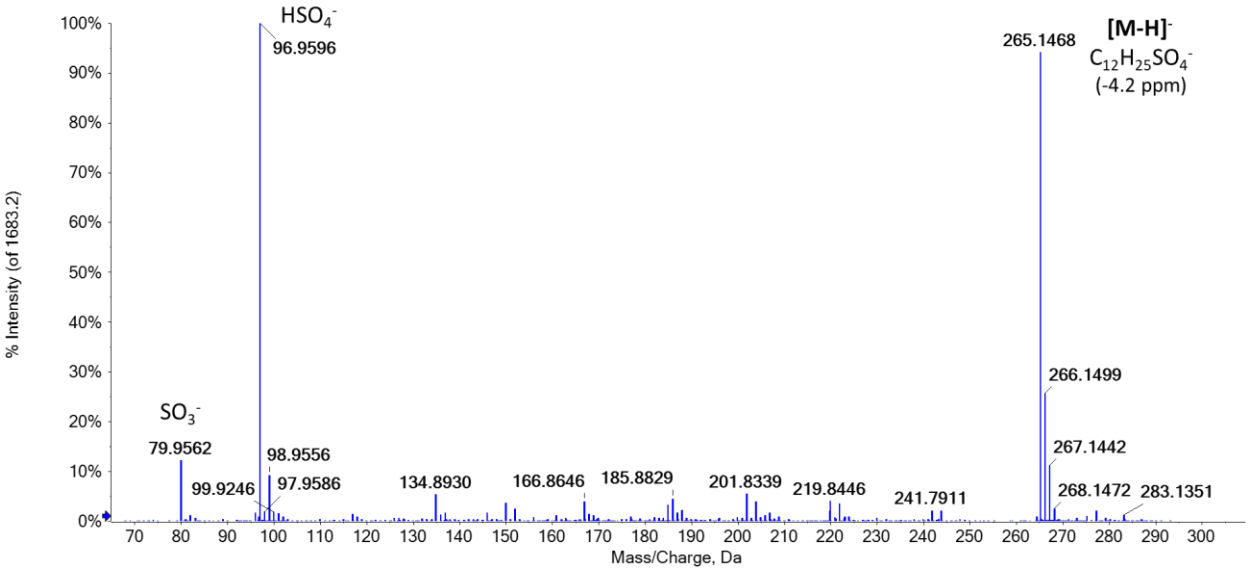


**Figure S1-20.** Tandem mass spectrum of *m/z* 265.1476 at $t_R$ 12.2 min of compound **18**, annotated in methanolic root extracts of *Lumnitzera littorea* and *L. racemosa*. The spectrum was acquired with a QqTOF mass spectrometer operated in the negative SWATH mode (*m/z* window 264.0–290.0).

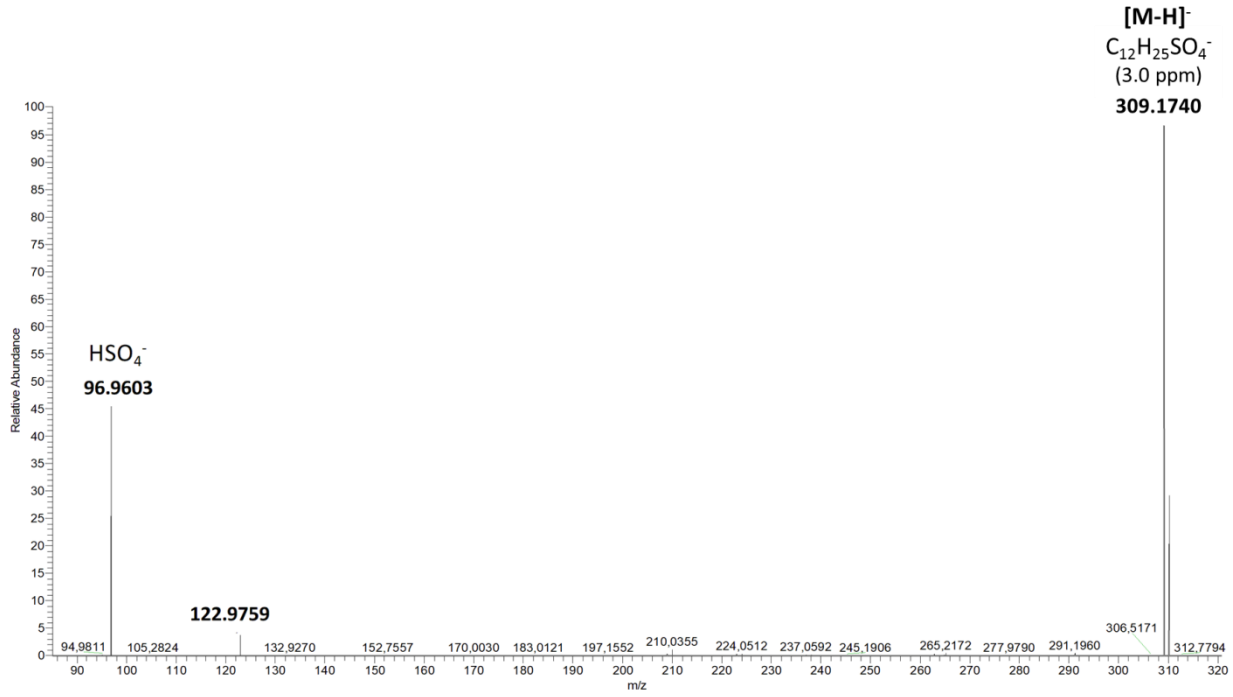


**Figure S1-21.** Tandem mass spectrum of *m/z* 309.1733 at $t_R$ 13.4 min of compound **19**, annotated in methanolic root extracts of *L. littorea* and *L. racemosa*. The spectrum was acquired with LIT-Orbitrap-MS in negative ion mode with CID activation (35% relative collision energy).

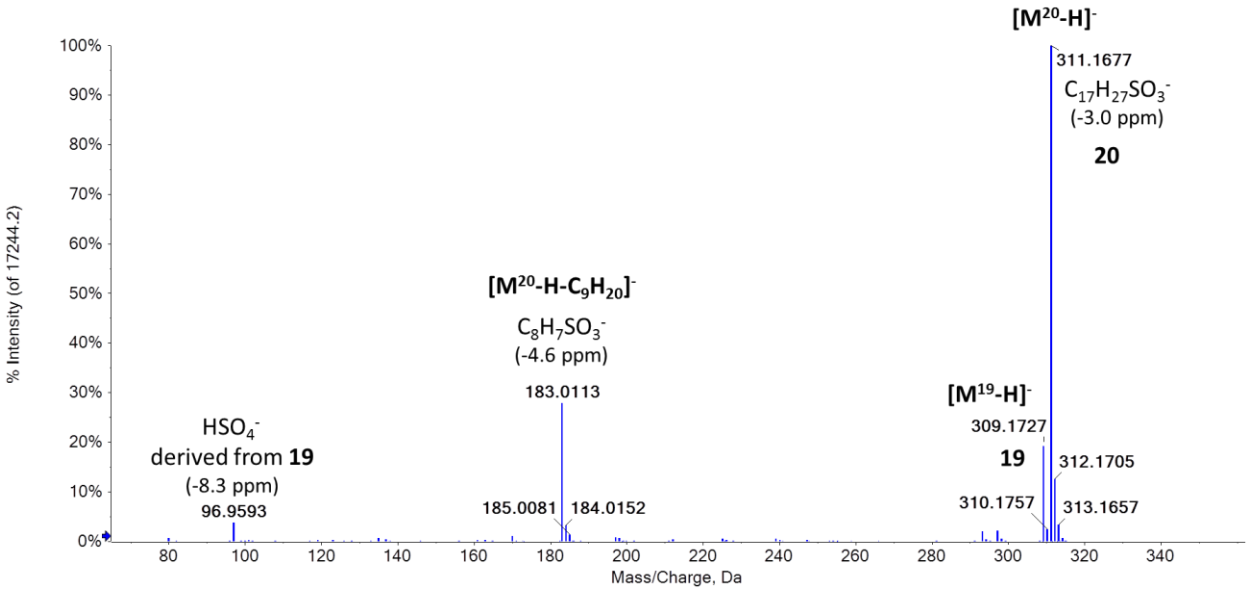


**Figure S1-22.** Tandem mass spectrum of *m/z* 309.1733 and 311.1685 at $t_R$ 13.4 min of compounds **19** and **20**, respectively, annotated in methanolic root extracts of *Lumnitzera littorea* and *L. racemosa*. The spectrum was acquired with a QqTOF mass spectrometer operated in the negative SWATH mode (*m/z* window 289.0–315.0).

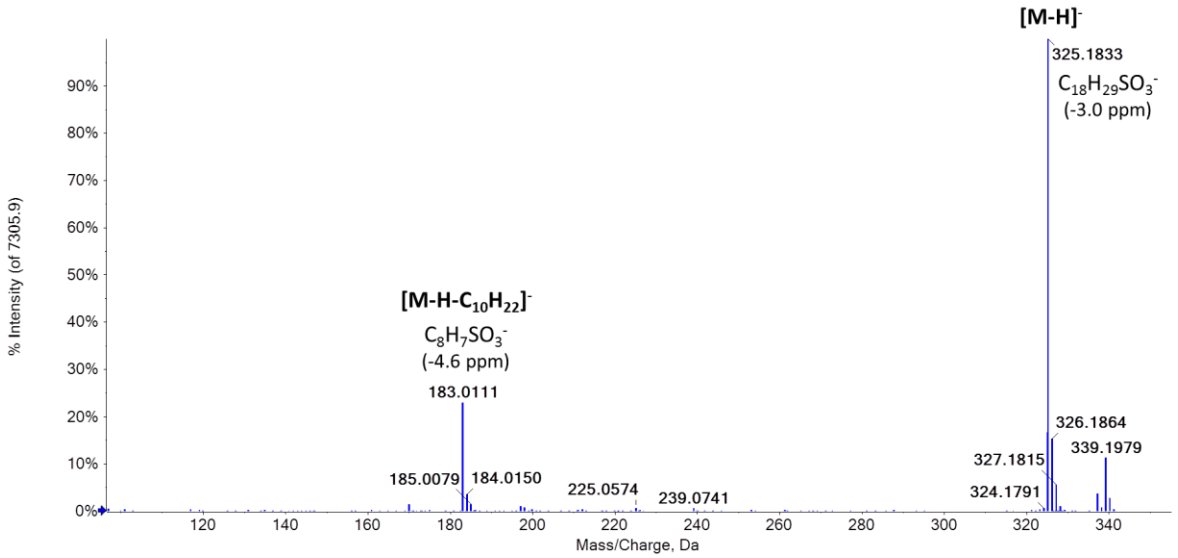


**Figure S1-23.** Tandem mass spectrum of *m/z* 325.1833 at $t_R$ 14.6 min of compound **21**, annotated in methanolic root extracts of *Lumnitzera littorea* and *L. racemosa*. The spectrum was acquired with a QqTOF mass spectrometer operated in the negative SWATH mode (*m/z* window 314.0–340.0).

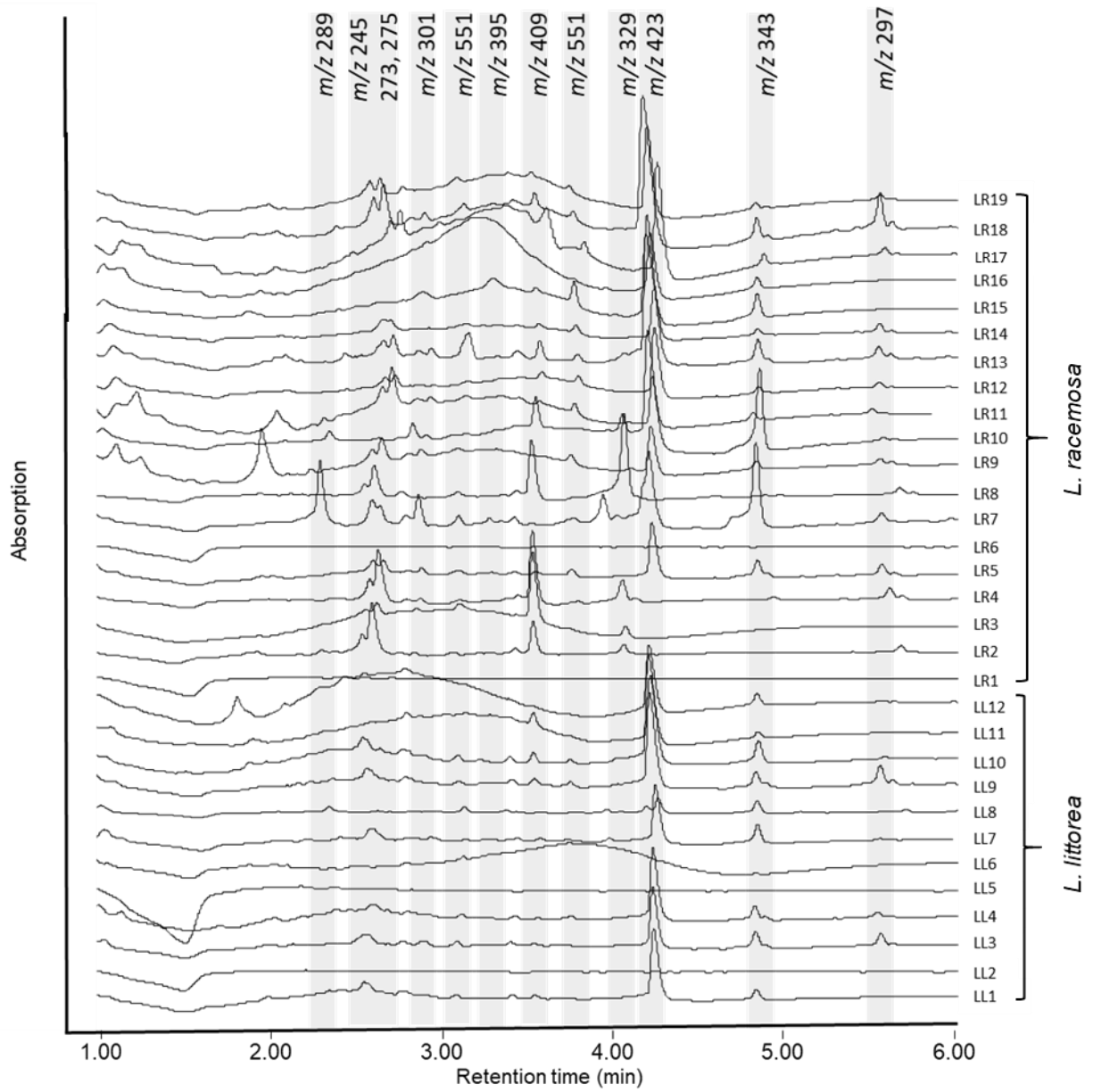


**Figure S2.** PDA chromatogram (200-400 nm) of root extracts from *Lumnitzera littorea* (LL1-LL12) and *L. racemosa* (LR1-LR19) obtained by an ACQUITY UHPLC-ESI-Q-MS* system.

*UHPLC-ESI-Q-MS

Eluents A and B are water and acetonitrile, respectively, both containing 0.1% (v/v) formic acid. Samples (2 µL) were loaded on an Acquity UPLC Reversed-Phase Ethylene Bridged Hybrid (BEH) column (C18-phase, ID 1 mm, length 50 mm, particle size 1.7 µm, Waters GmbH, Eschborn, Germany) under isocratic conditions (95% eluent A, 5% B, 2 min), and separated using a linear gradient from 5 to 90% eluent B in 9 min. Separation was performed on an ACQUITY UPLC I-Class UHPLC System (Waters GmbH, Eschborn, Germany) with a flow rate of 0.4 mL/min and 40 °C column temperature. The column effluents were introduced on-line into a photodiode array detector (Waters PDA eλ, 200 – 400 nm, sampling rate 10 Hz, 4.8 nm) and further in a Waters QDa quadrupole mass spectrometer, operated in a mass detector/negative ion mode. MS data were acquired in a negative scan mode with a target sampling rate of 8 points/second. Cone voltage was set to -15 V, capillary voltage to -0.8 kV.

**Tab. S1.** Peak areas (presented as counts per second) of main compounds integrated in total ion chromatograms (TIC) acquired for root extracts of *Lumnitzera littorea* (LL1-LL12) and *L. racemosa* (LR1-LR19) by UHPLC-ESI-Q-MS.

| **Compound** | **2** | **4** | **3** | **6** | **7** | **9** | **10** | **13** | **15** | **16** |
|---|---|---|---|---|---|---|---|---|---|---|
| **rt (min)** | 2,5 | 2,55 | 2,6 | 2,8 | 3,25 | 3,5 | 3,7 | 4.0 | 4,2 | 4,8 |
| ***m/z*** | 245 | 275 | 273 | 301 | 395 | 409 | 551 | 329 | 423 | 343 |
| LL1 | 16305 | | | | | 6238 | | | 110995 | 16608 |
| LL2 | no results | | | | | | | | | |
| LL3 | 13630 | | | 1513 | | 122511 | | | 114942 | 22498 |
| LL4 | 24579 | | | | | 4649 | | | 88144 | 22967 |
| LL5 | no results | | | | | | | | | |
| LL6 | no results | | | | | | | | | |
| LL7 | | | | 6535 | | 5462 | | | 106017 | 36740 |
| LL8 | 3789 | | | | | 1057 | | 2670 | 40123 | 37841 |
| LL9 | 21145 | | | | | 9796 | | | 151009 | 23011 |
| LL10 | 25221 | | 4150 | | | 16614 | | | 198140 | 40378 |
| LL11 | | 3748 | | 2550 | 12559 | 28413 | 2299 | | 151567 | 13810 |
| LL12 | 6384 | | | | | 3478 | | | 149719 | 26341 |
| LR1 | no results | | | | | | | | | |
| LR2 | | | 78929 | 4551 | | 56839 | | 18648 | - | - |
| LR3 | 2505 | 1491 | | 5236 | 3122 | 122511 | | 19629 | - | - |
| LR4 | | | 79472 | 7763 | | 138091 | | 40885 | - | - |
| LR5 | | 15620 | 14988 | 10647 | 2798 | 6100 | 15731 | 1745 | 109580 | 33141 |
| LR6 | no results | | | | | | | | | |
| LR7 | | 81480 | | 51234 | | 1907 | | 51480 | 169288 | 159443 |
| LR8 | | | 53366 | | | 129533 | | 192405 | - | - |
| LR9 | 2960 | | 36775 | 12512 | | | 19070 | | 104486 | 18387 |
| LR10 | | 5159 | | 7683 | 2742 | 62649 | 4764 | 38071 | 268823 | 176536 |
| LR11 | | | 51202 | 8262 | | 5296 | 19239 | | 89767 | trace |
| LR12 | | 12224 | 14599 | 2868 | 3528 | 13273 | 15569 | | 135585 | 13301 |
| LR13 | | | 24944 | | | 34692 | 14871 | 5170 | 321378 | 43682 |
| LR14 | | 73803 | | | | 8577 | 15843 | | 103275 | 12378 |
| LR15 | | 12486 | | | 37950 | 13877 | 58091 | | 253222 | 64018 |
| LR16 | | | | 6150 | | 3113 | 5317 | | 151301 | 30436 |
| LR17 | | 9662 | 29179 | 6747 | 8754 | 52981 | 22757 | | 193709 | 18905 |
| LR18 | 15725 | | 58754 | 12312 | 8944 | 27402 | 17967 | | 340237 | 42964 |
| LR19 | | 22624 | 22765 | | | 8366 | 8810 | | 224365 | 9920 |

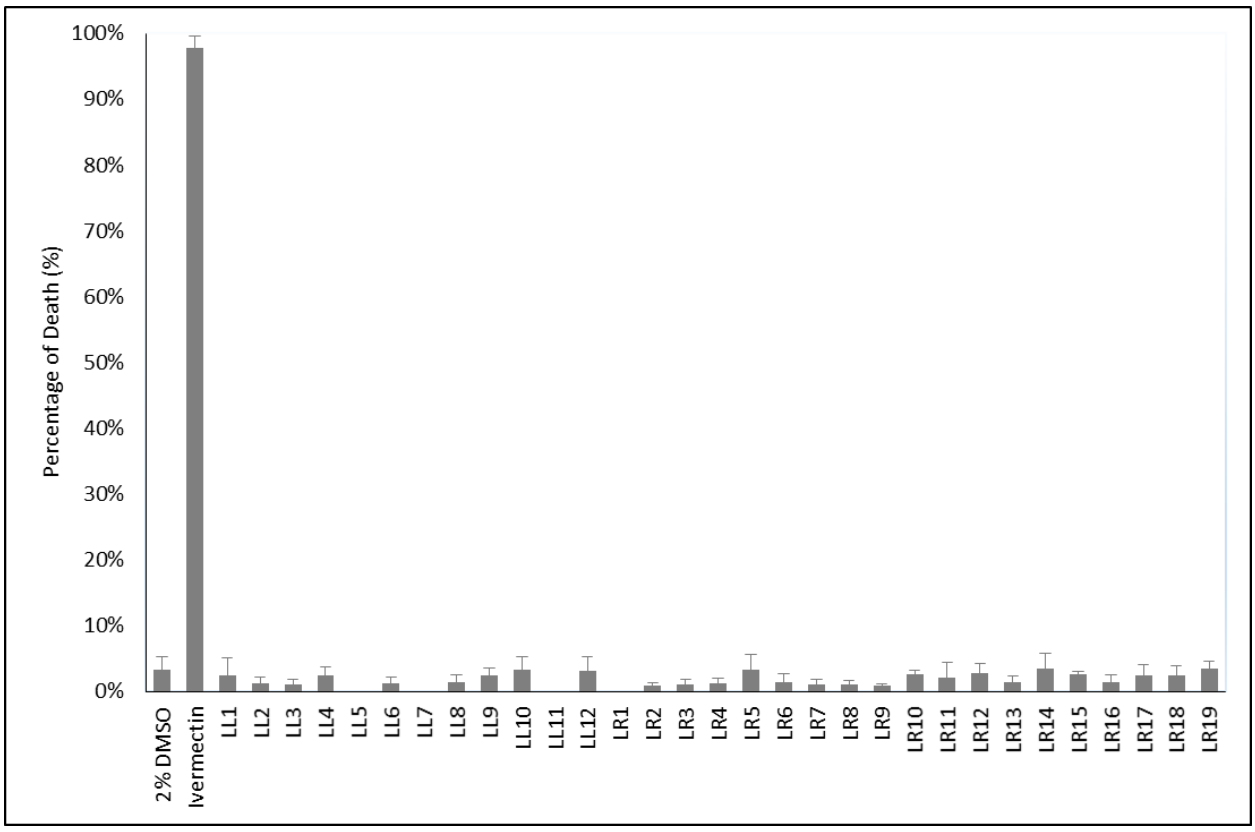


**Figure S3.** Anthelmintic activity of root extracts from *Lumnitzera littorea* (LL1-LL12) and *L. racemosa* (LR1-LR19) at the concentration of 500 µg/ml against *Caenorhabditis elegans*. The solvent DMSO (2% v/v) and the standard anthelmintic drug ivermectin (10 µg/mL, 100% dead worms after 30 min incubation) were used as negative and positive controls, respectively. Results are given as percentage of dead worms.

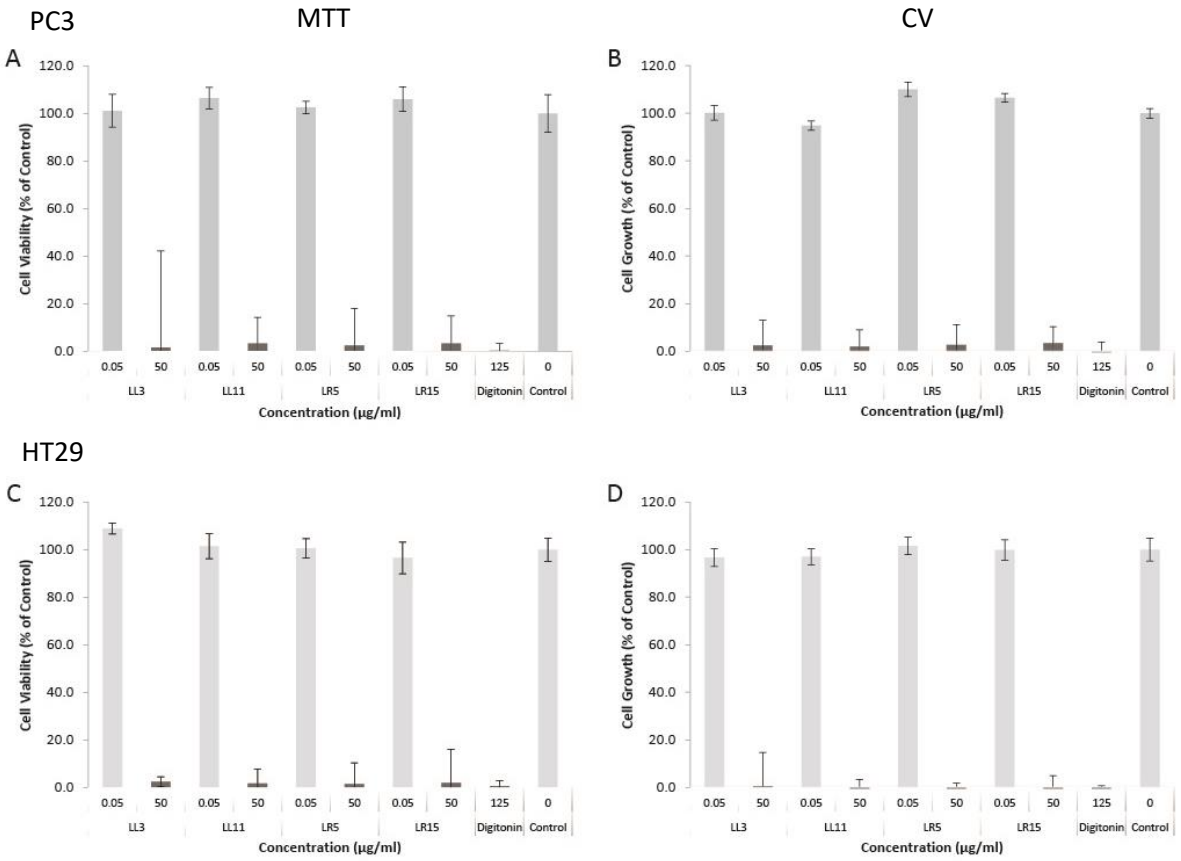


**Figure S4.** Cytotoxic activity of root extracts from *Lumnitzera littorea* (LL3, LL11) and *L. racemosa* (LR5, LR15) against the human prostate cancer cell line PC3 (A and B) and the colon adenocarcinoma cell line HT29 (C and D) determined by MTT (A, C) and CV assays (B, D). Digitonin (125 µg/mL) was used as positive control. The results are given as percentage of control values without treatment (= 100%).

**Table S2.** NMR spectroscopic data (400 MHz, methanol-d4) for 4-(4-hydroxyphenyl)-2-butanol 2-*O*-sulfate (**2**).

| position | $\delta_C$[a], type | $\delta_H$ (J in Hz) | COSY | HMBC |
|---|---|---|---|---|
| 1 | 21.2, $CH_3$ | 1.33, d (6.3) | 2 | 2, 3 |
| 2 | 76.8, CH | 4.46, m | 1, 3a,b | |
| 3 | 40.5, $CH_2$ | 1.89 (3a), m | 2, 4 | 2 |
| | | 1.75 (3b), m | | 1, 2, 4, 1′ |
| 4 | 31.8, $CH_2$ | 2.55-2.70, m | 3a,b | 2, 3, 1′, 2′, 6′ |
| 1′ | 134.6[b], C | | | |
| 2′ | 130.3, CH | 7.03, d-like (8.4) | 3′ | 4, 4′, 6′ |
| 3′ | 116.1, CH | 6.67, d-like (8.4) | 2 | 1′, 4′, 5′ |
| 4′ | 156.4[b], C | | | |
| 5′ | 116.1, CH | 6.67, d-like (8.4) | 6′ | 1′, 3′, 4′ |
| 6′ | 130.3, CH | 7.03, d-like (8.4) | 5′ | 4, 2′, 4′ |

[a] derived from HSQC or [b] HMBC

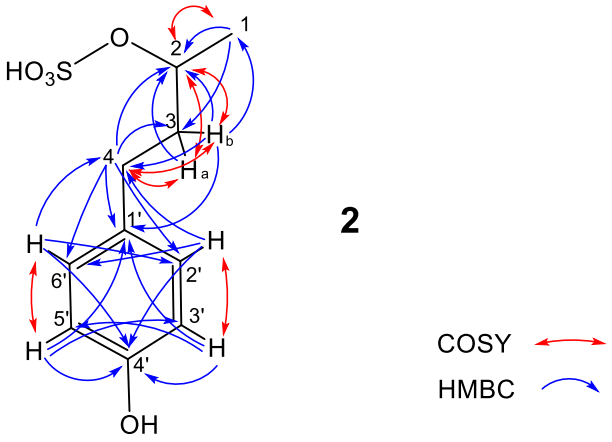

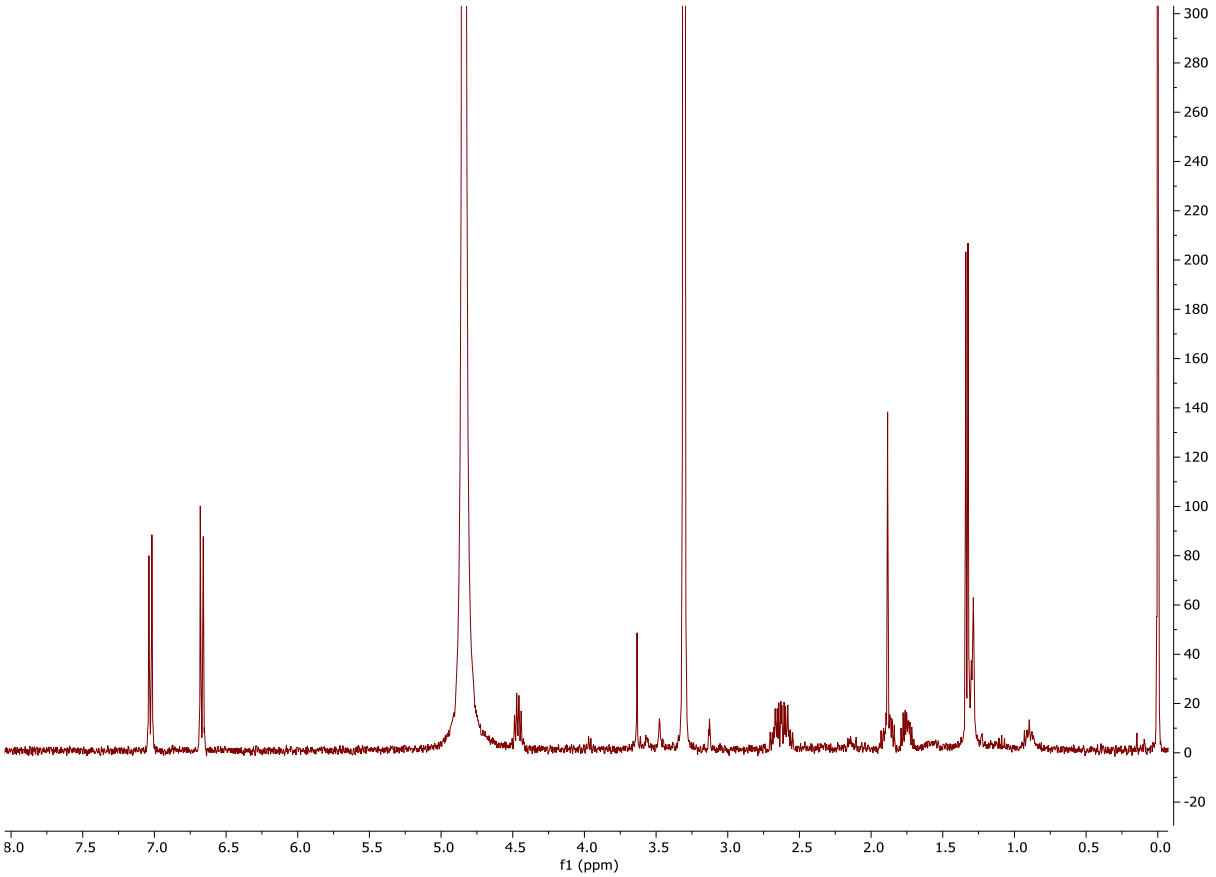


**Figure S5-1.** $^{1}$H NMR spectrum of 4-(4-hydroxyphenyl)-2-butanol 2-*O*-sulfate (**2**).

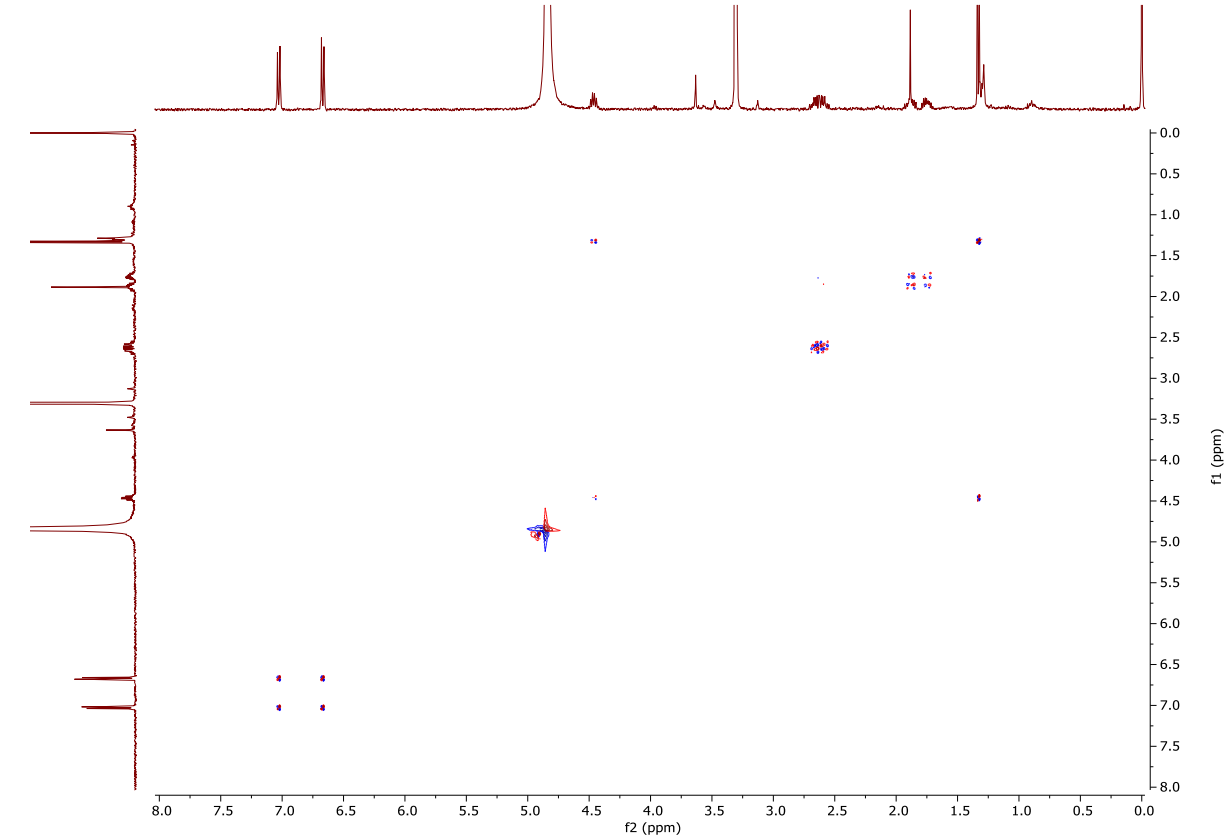


**Figure S5-2.** COSY spectrum of 4-(4-hydroxyphenyl)-2-butanol 2-*O*-sulfate (**2**).

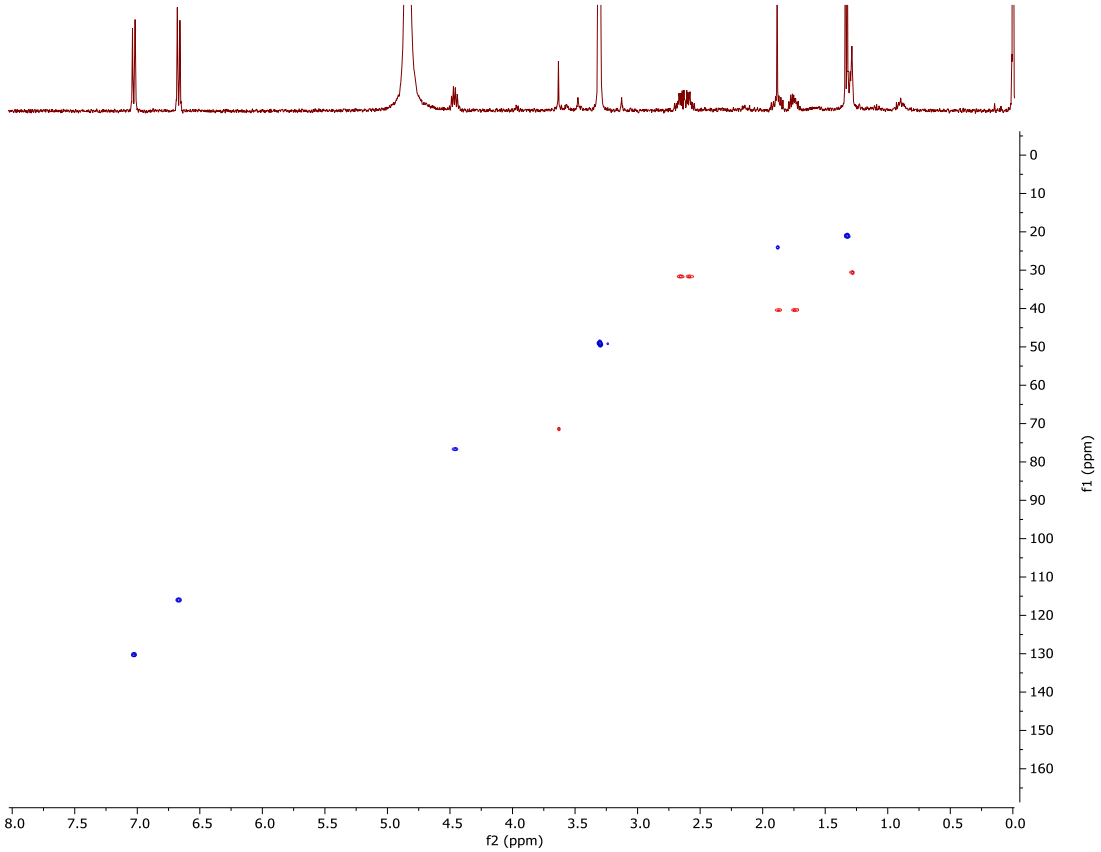


**Figure S5-3.** HSQC spectrum of 4-(4-hydroxyphenyl)-2-butanol 2-*O*-sulfate (**2**).

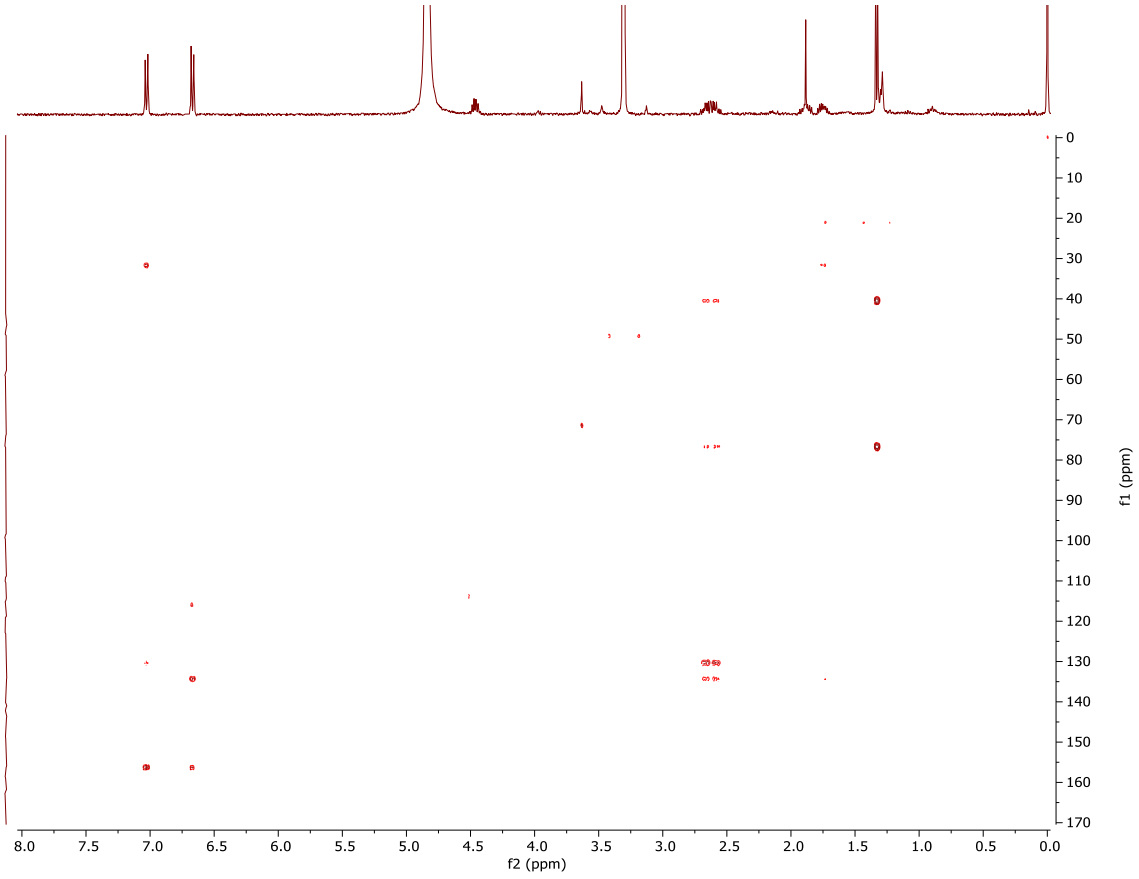


**Figure S5-4.** HMBC spectrum of 4-(4-hydroxyphenyl)-2-butanol 2-*O*-sulfate (**2**).

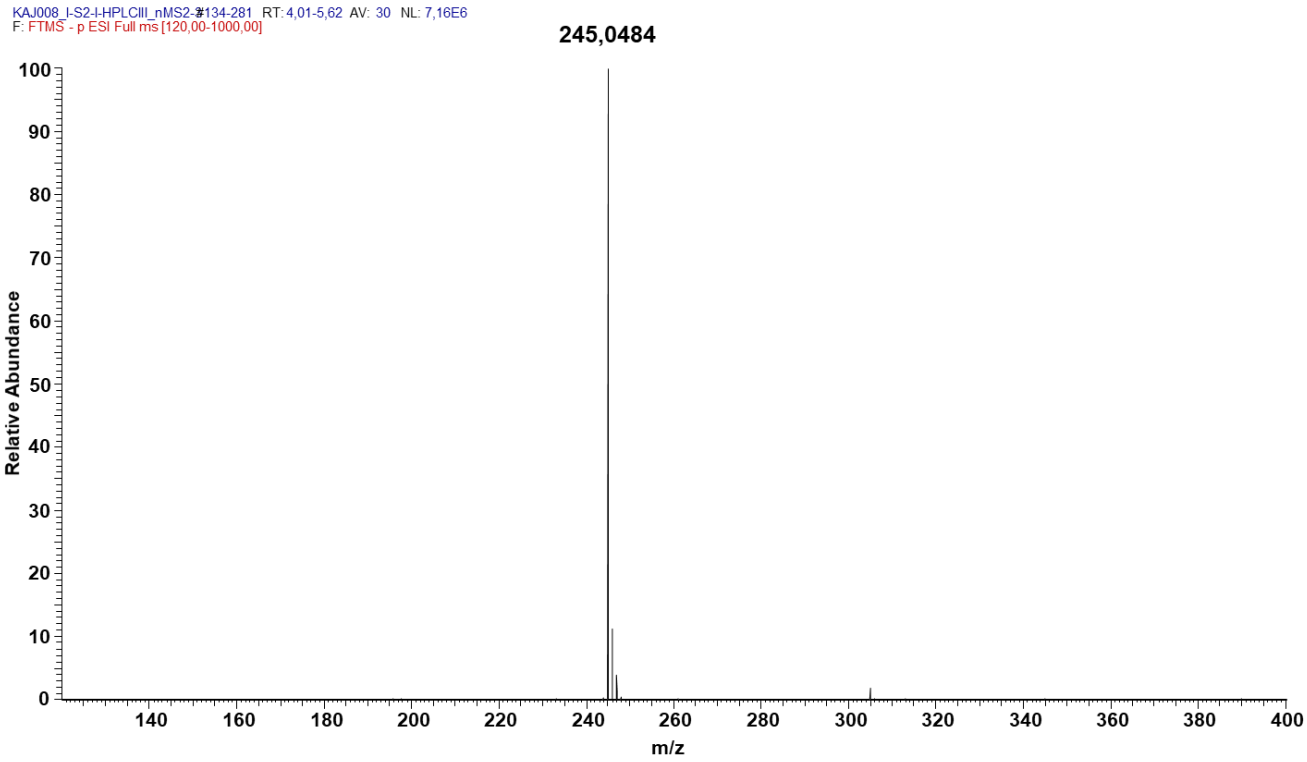


**Figure S5-5.** Full HRMS spectrum of 4-(4-hydroxyphenyl)-2-butanol 2-*O*-sulfate (**2**) acquired with LIT-Orbitrap-MS in negative ion mode.

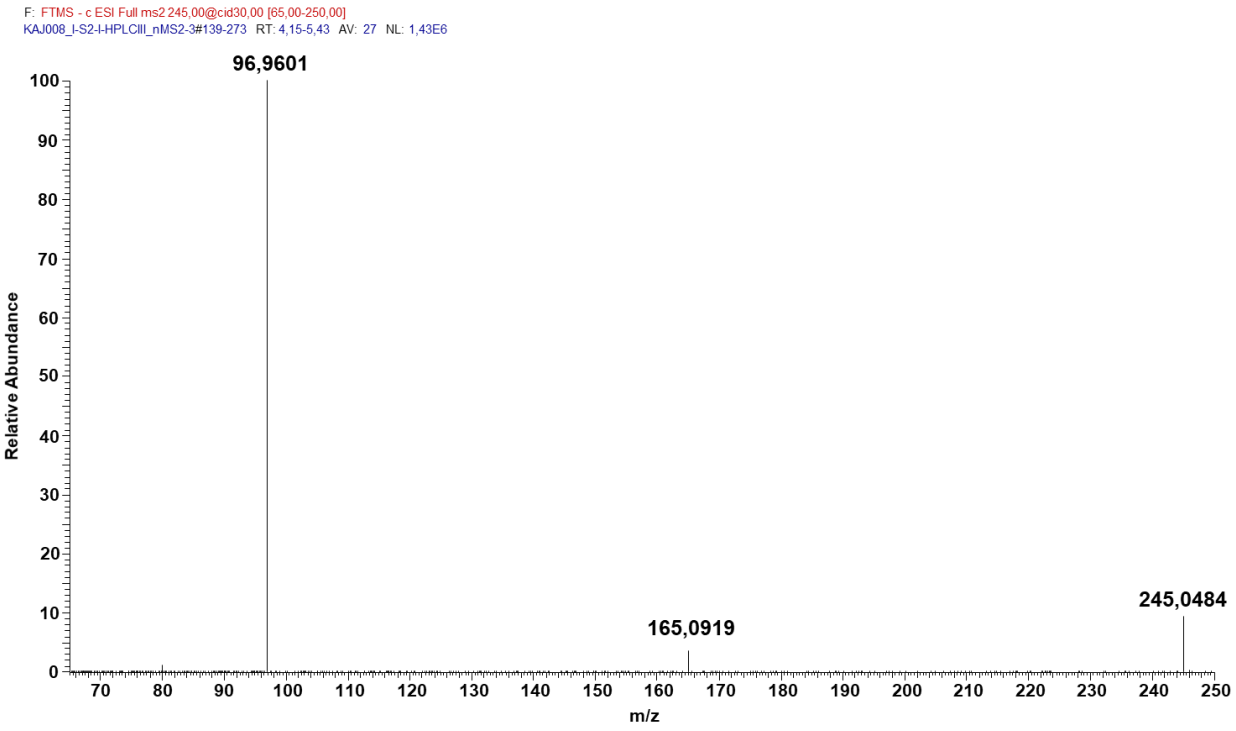


**Figure S5-6.** MS2 spectrum of 4-(4-hydroxyphenyl)-2-butanol 2-*O*-sulfate (**2**) acquired with LIT-Orbitrap-MS in negative ion mode with CID activation (30% relative collision energy).

**Table S3.** NMR spectroscopic data (400 MHz, methanol-d4) for 4-(4-sulfoxy-3-methoxyphenyl)-butan-2-one (**3**).

| position | $\delta_C$, type | $\delta_H$ (J in Hz) | COSY | HMBC |
|---|---|---|---|---|
| 1 | 30.06, $CH_3$ | 2.11, s | 3 | 2, 3 |
| 2 | 211.47, C=O | | | |
| 3 | 46.30, $CH_2$ | 2.76, s | 1, 4 | 2, 4 |
| 4 | 30.55, $CH_2$ | 2.76, s | 3 | 3, 1′, 2′, 6′ |
| 1′ | 134.02, C | | | |
| 2′ | 113.14, CH | 6.77, d (2.0) | 6′ | 4, 3′, 4′, 6′ |
| 3′ | 148.96, C | - | | |
| 4′ | 145.85, C | - | | |
| 5′ | 116.20, CH | 6.68, d (8.0) | 6′ | 1′, 3′, 4′, |
| 6′ | 121.70, CH | 6.61, dd (8.0, 2.0) | 2′, 5′ | 4, 2′, 4′ |
| 3′-OMe | 56.39, $CH_3$ | 3.82, s | | 3′ |

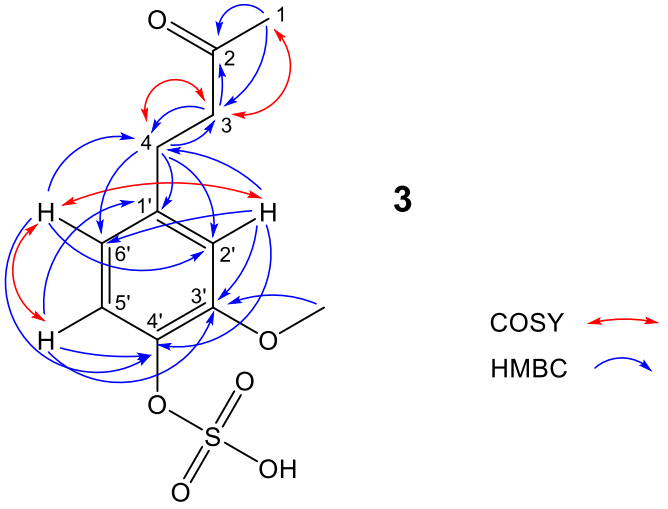

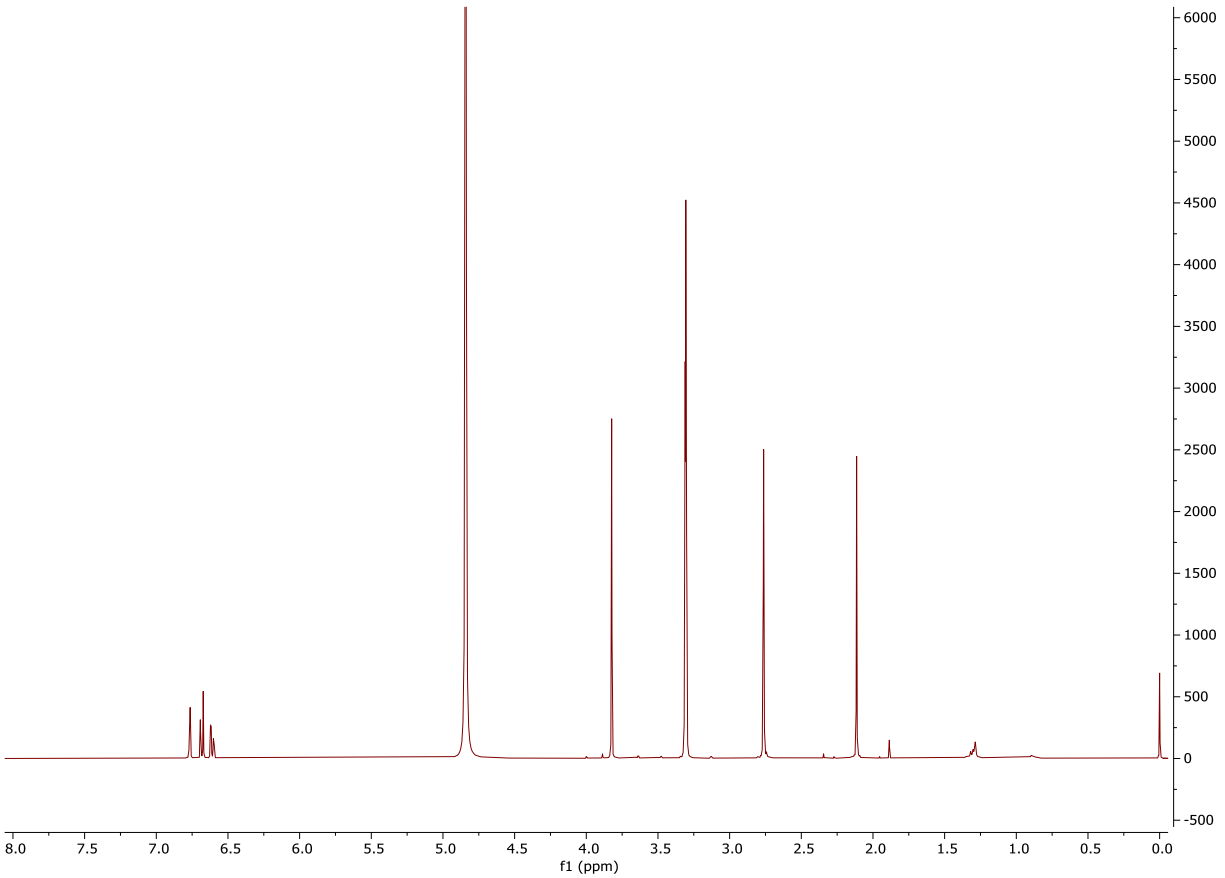


**Figure S6-1.** $^{1}$H NMR spectrum of 4-(4-sulfoxy-3-methoxyphenyl)-butan-2-one (**3**).

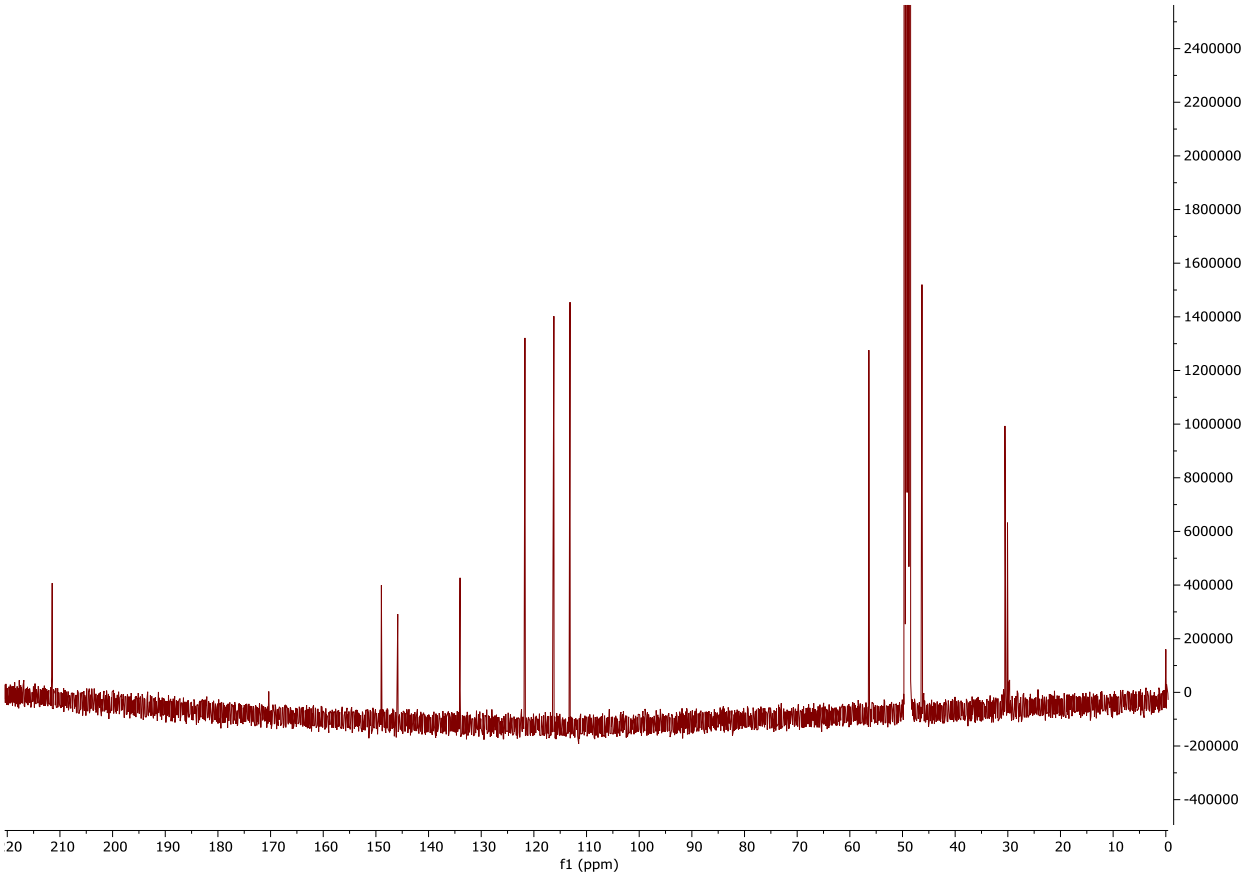


**Figure S6-2.** $^{13}$C NMR spectrum of 4-(4-sulfoxy-3-methoxyphenyl)-butan-2-one (**3**).

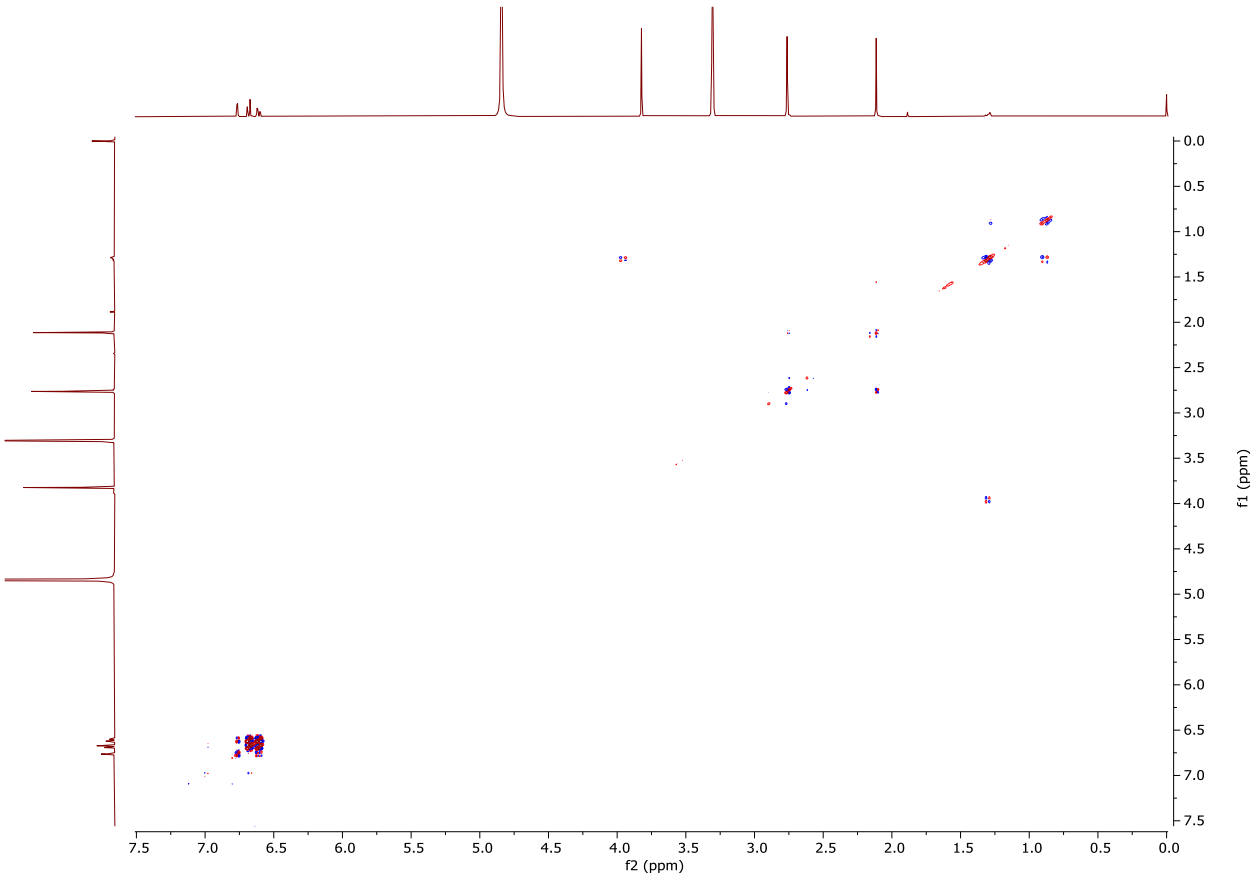


**Figure S6-3.** COSY spectrum of 4-(4-sulfoxy-3-methoxyphenyl)-butan-2-one (**3**).

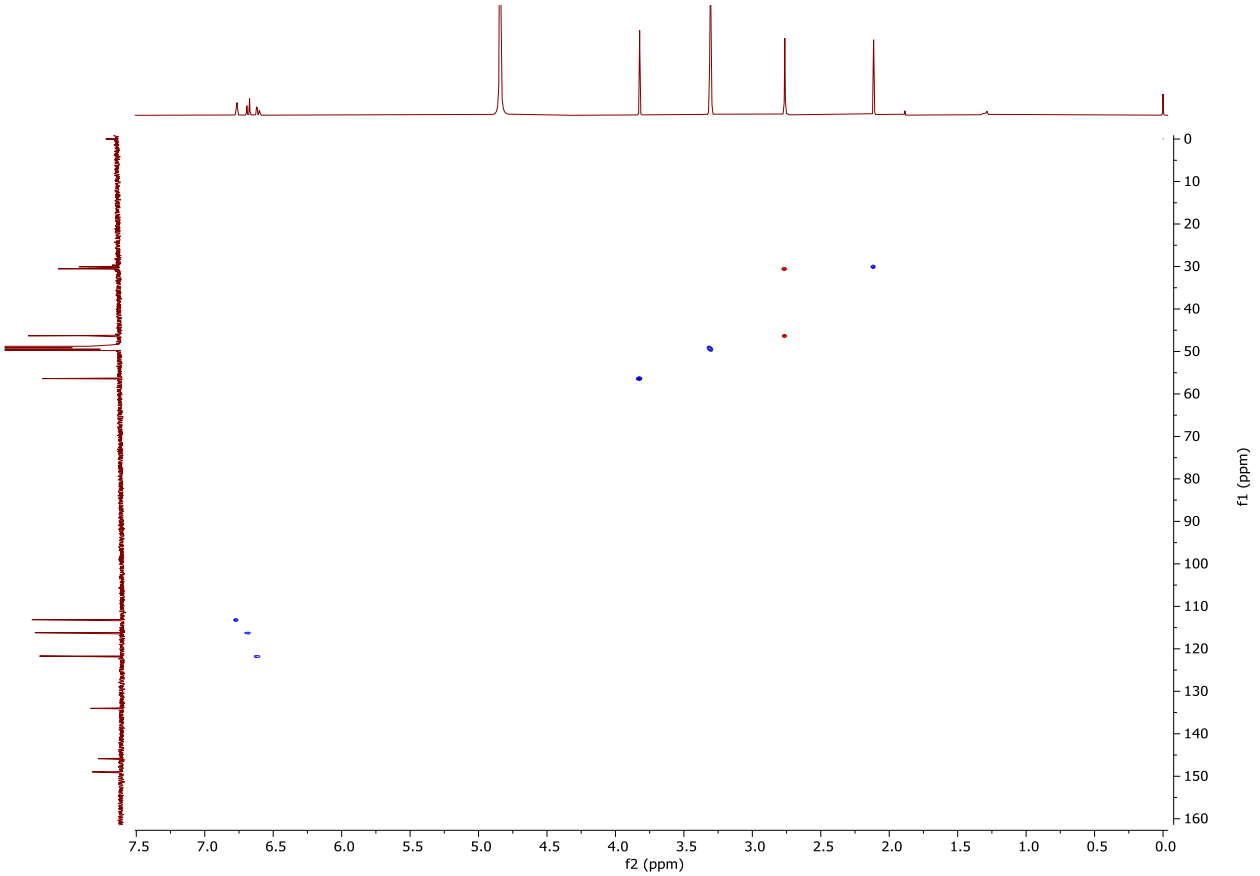


**Figure S6-4.** HSQC spectrum of 4-(4-sulfoxy-3-methoxyphenyl)-butan-2-one (**3**).

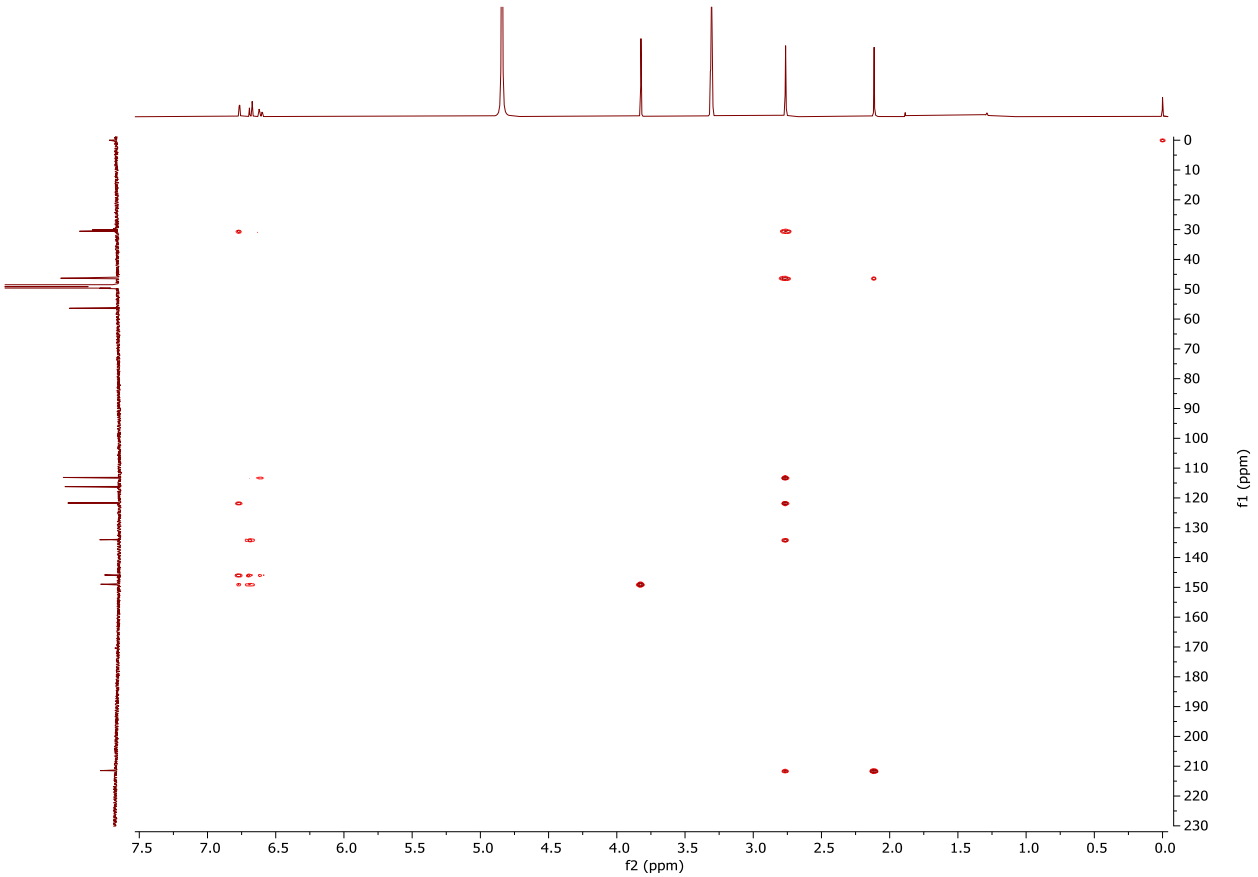


**Figure S6-5.** HMBC spectrum of 4-(4-sulfoxy-3-methoxyphenyl)-butan-2-one (**3**).

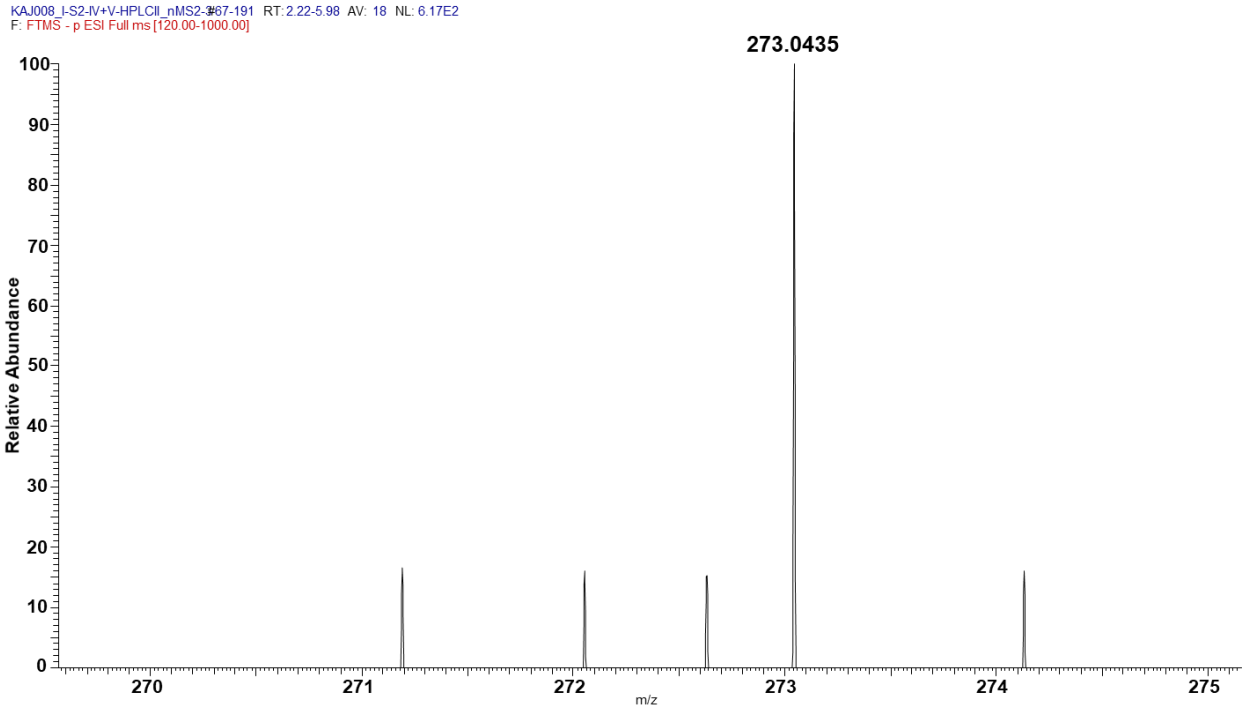


**Figure S6-6.** Full HRMS spectrum of 4-(4-sulfoxy-3-methoxyphenyl)-butan-2-one (**3**) acquired with LIT-Orbitrap-MS in negative ion mode.

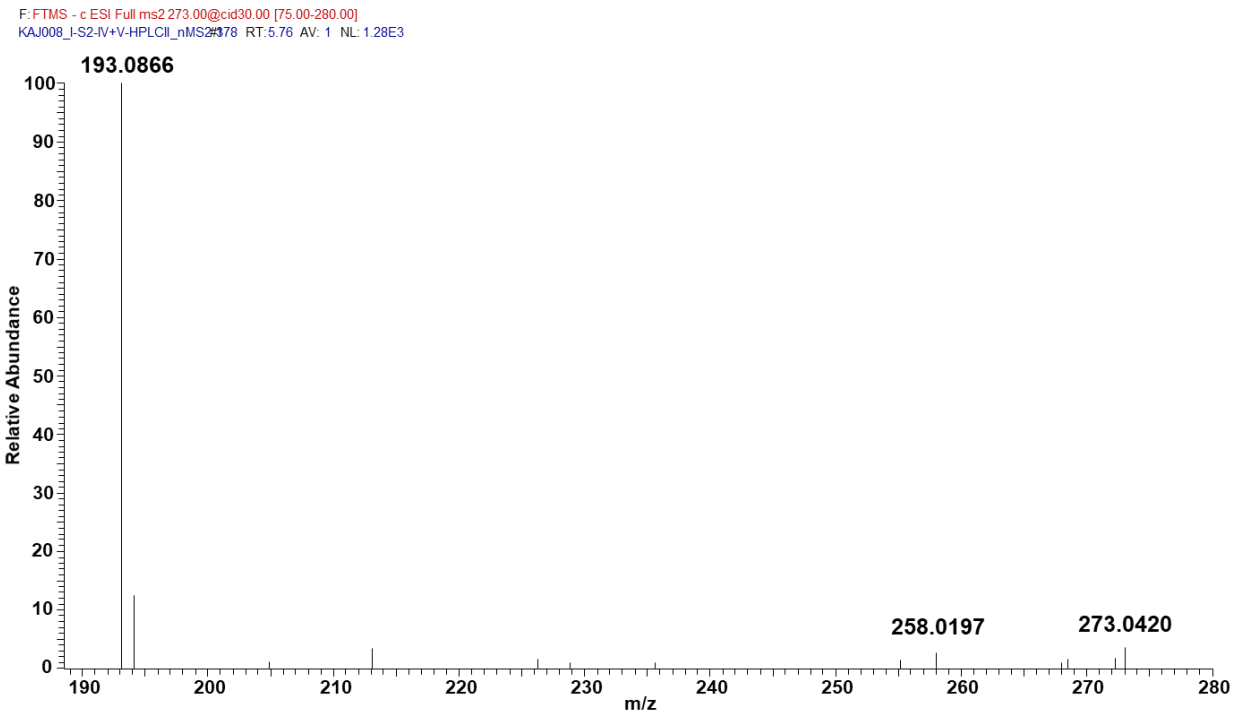


**Figure S6-7.** MS2 spectrum of 4-(4-sulfoxy-3-methoxyphenyl)-butan-2-one (**3**) acquired with LIT-Orbitrap-MS in negative ion mode with CID activation (30% relative collision energy).

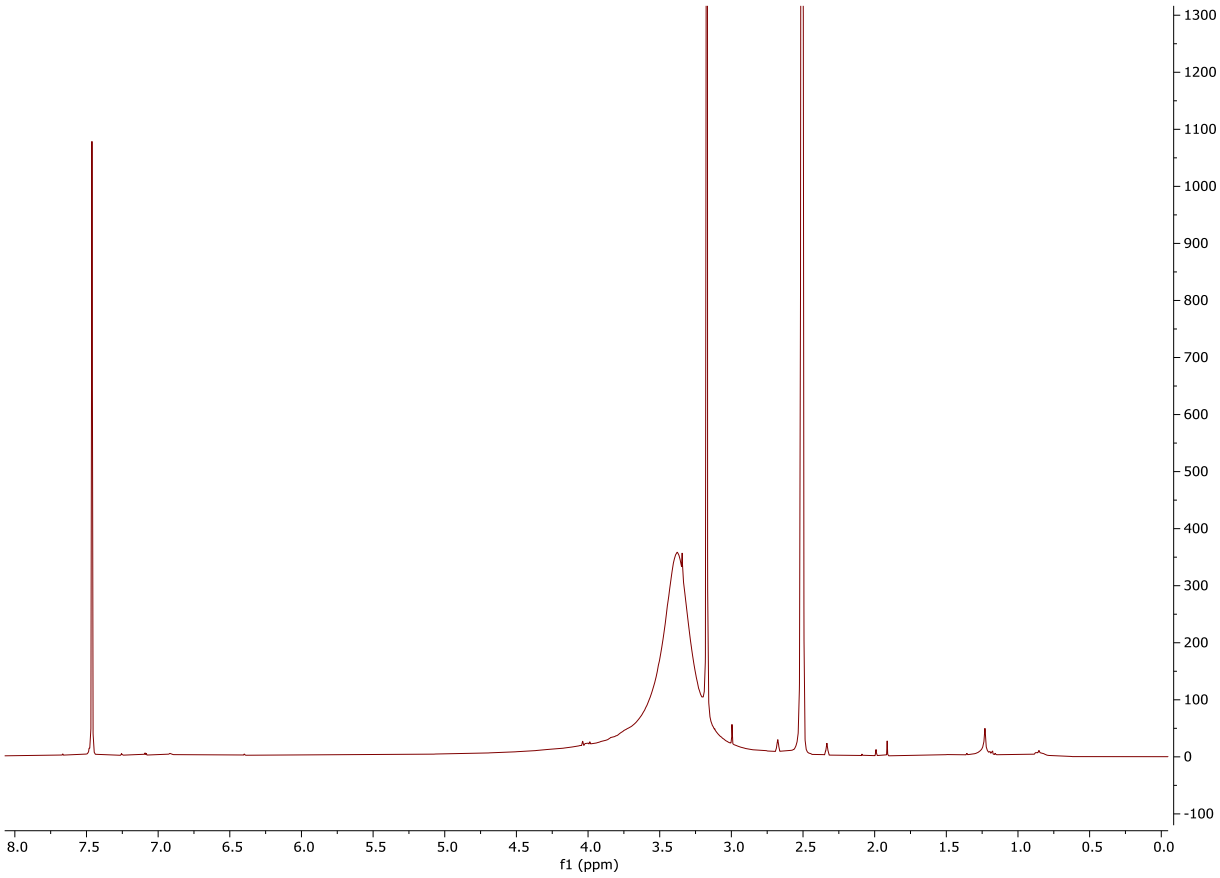


**Figure S7-1.** $^{1}$H NMR spectrum (DMSO-d6) of ellagic acid (**6**).

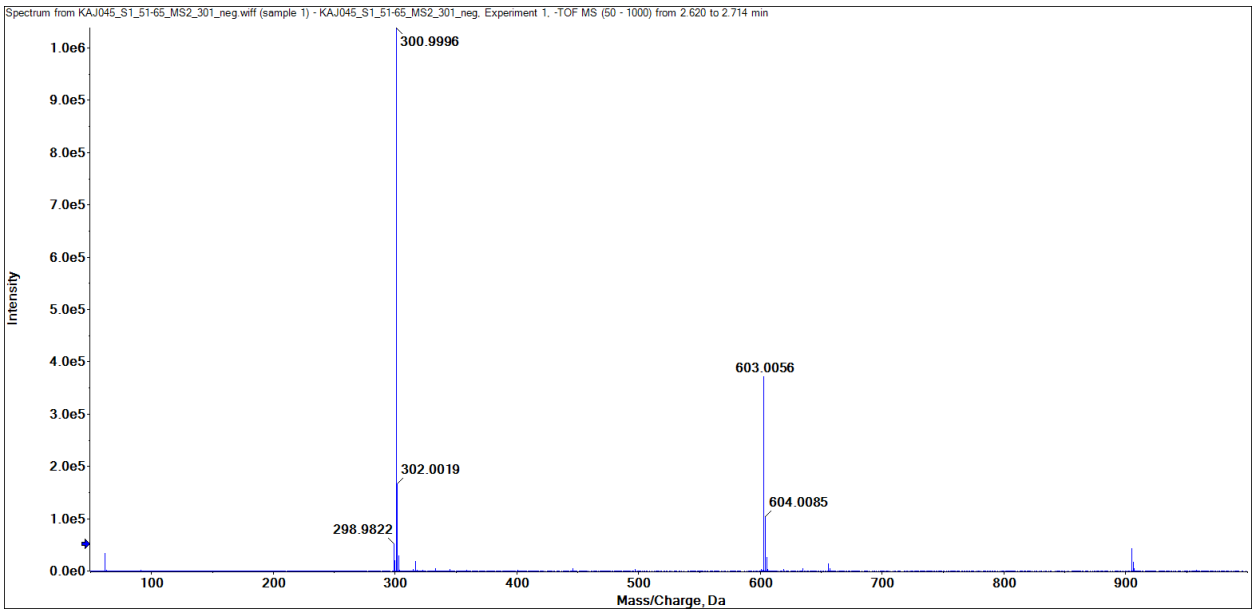


**Figure S7-2.** HRMS spectrum of ellagic acid (**6**) acquired with a QqTOF mass spectrometer in negative ion mode.

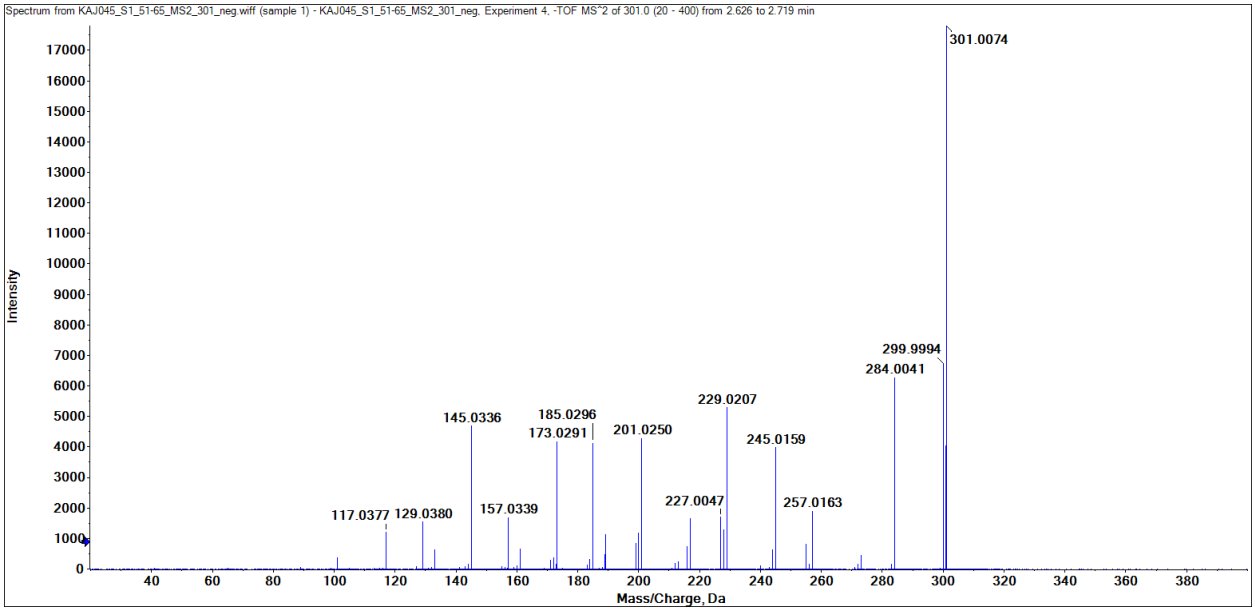


**Figure S7-3.** MS2 spectrum of ellagic acid (**6**) acquired with a QqTOF mass spectrometer in negative ion mode.

**Table S4.** NMR spectroscopic data (600 MHz, DMSO-d6) for 3,4-di-*O*-methylellagic acid (**13**).

| position | $\delta_H$ (J in Hz) | $\delta_C$ *, type | HMBC | ROESY |
|---|---|---|---|---|
| 1 | | 115.00, C | | |
| 2 | | 141.79, C | | |
| 3 | | 140.04, C | | |
| 4 | | 152.73, C | | |
| 5 | 7.53, s | 105.83, CH | 1, 2, 3, 4, 6, 7 | 4-OMe |
| 6 | | 112.95, C | | |
| 7 | | 160.22, C | | |
| 1' | | 114.97, C | | |
| 2' | | 134.51, C | | |
| 3' | | 151.92, C | | |
| 4' | | 156.46, C | | |
| 5' | 7.09, s | 104.63, CH | 1', 2', 3', 4', 6', 7' | |
| 6' | | 113.09, C | 5' | |
| 7' | | 159.15, C | 5' | |
| 3-OMe | 3.99, s | 60.83, $CH_3$ | 3 | |
| 4-OMe | 3.97, s | 56.32, $CH_3$ | 4, 5 | 5 |

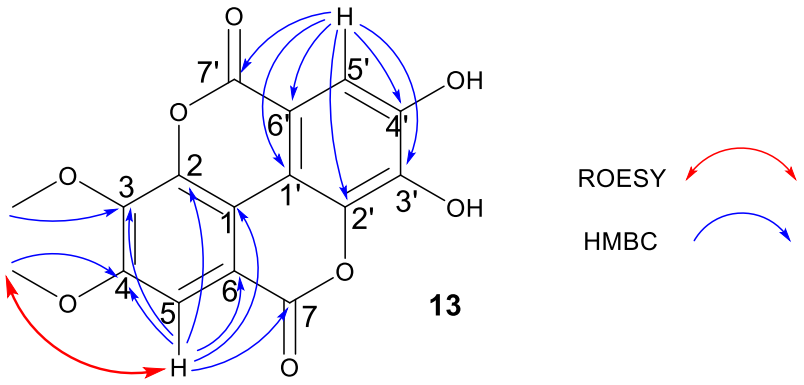

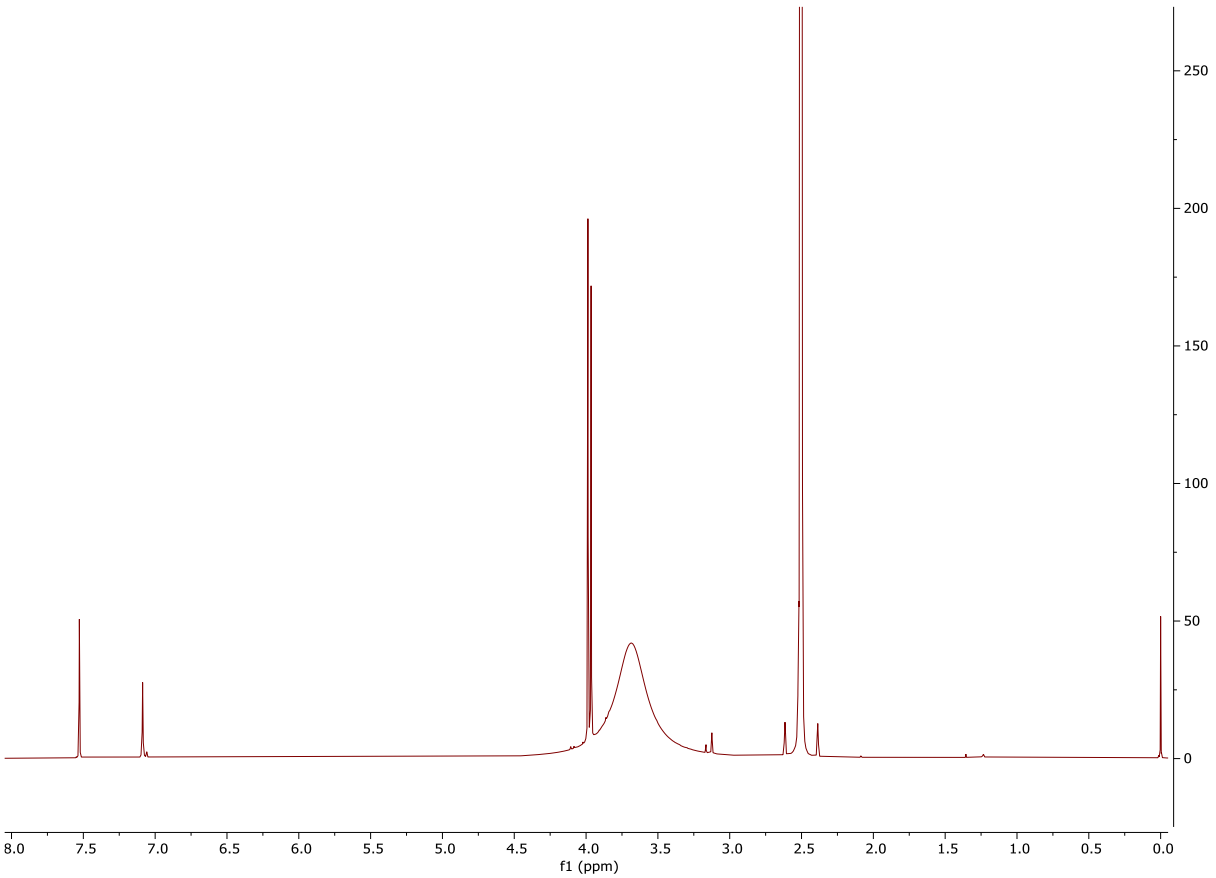


**Figure S8-1.** $^{1}$H NMR spectrum (DMSO-d6) of 3,4-di-*O*-methylellagic acid (**13**).

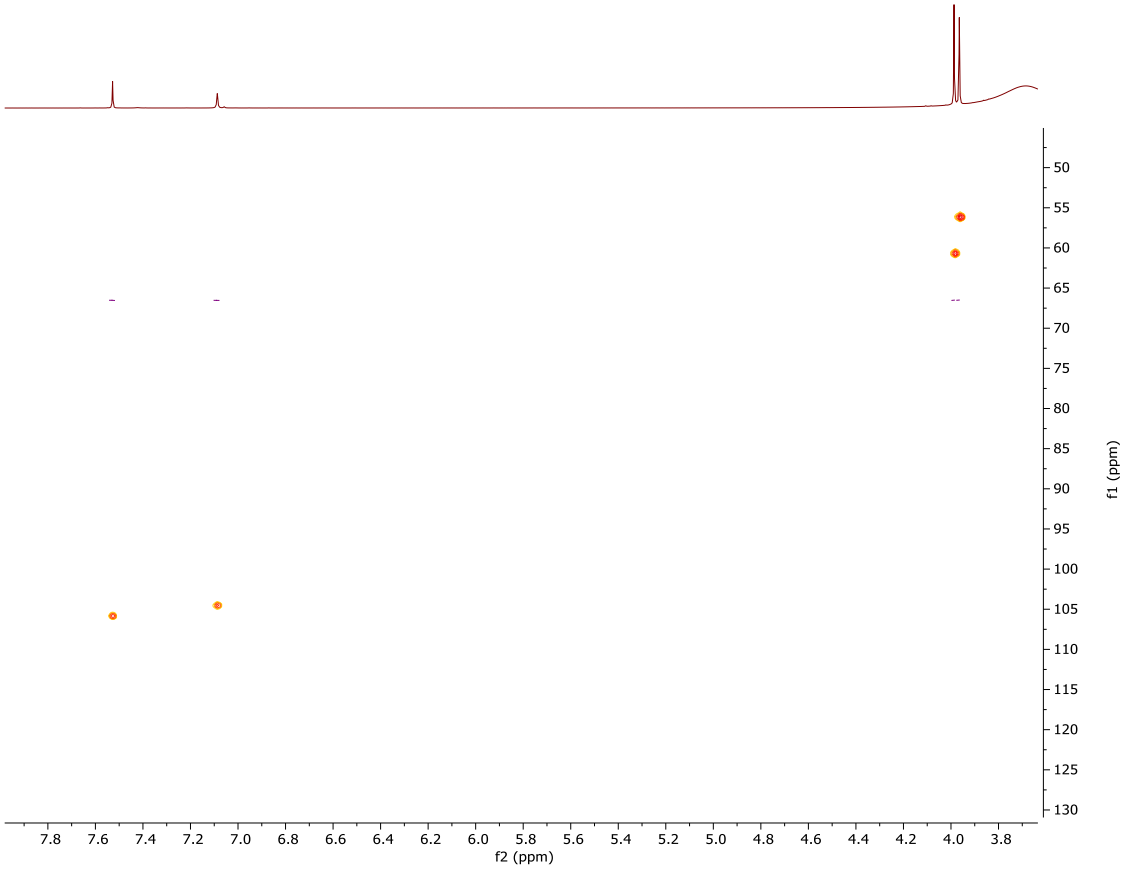


**Figure S8-2.** HSQC spectrum (DMSO-d6) of 3,4-di-*O*-methylellagic acid (**13**).

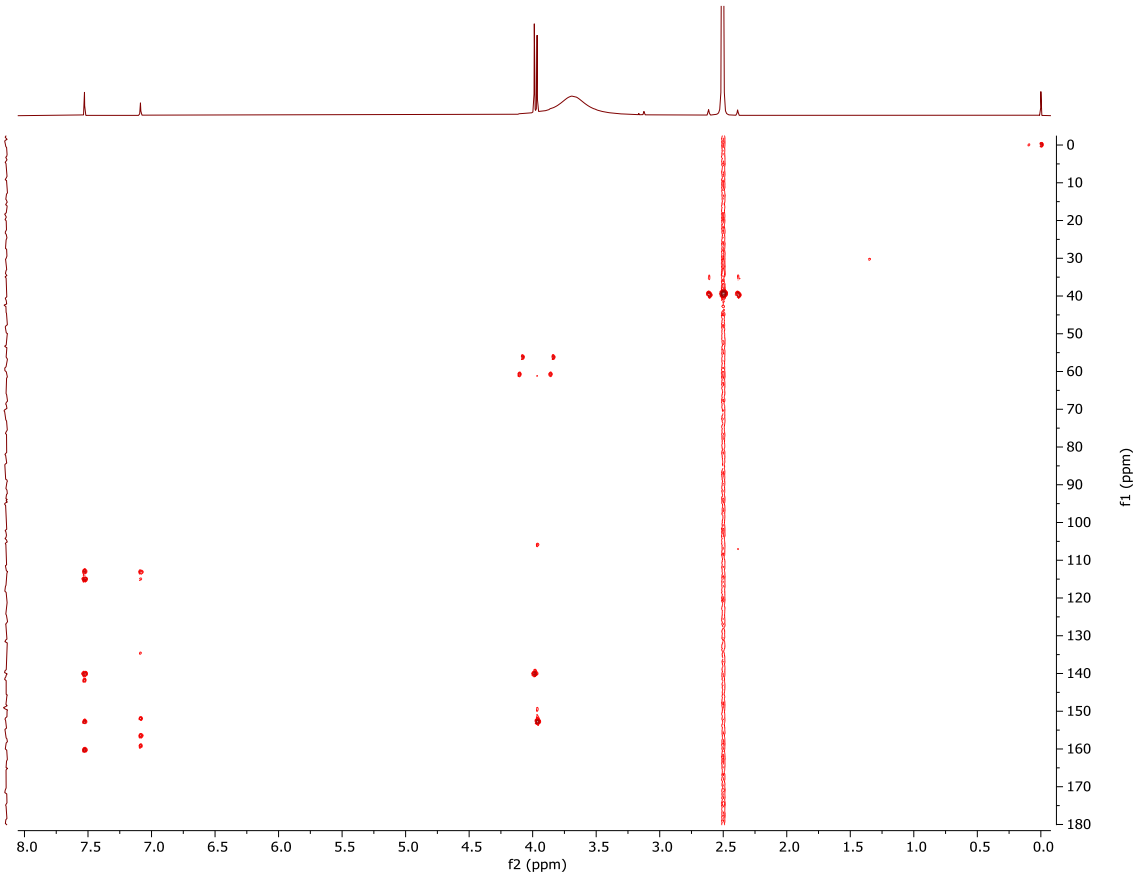


**Figure S8-3.** HMBC spectrum (DMSO-d6) of 3,4-di-*O*-methylellagic acid (**13**).

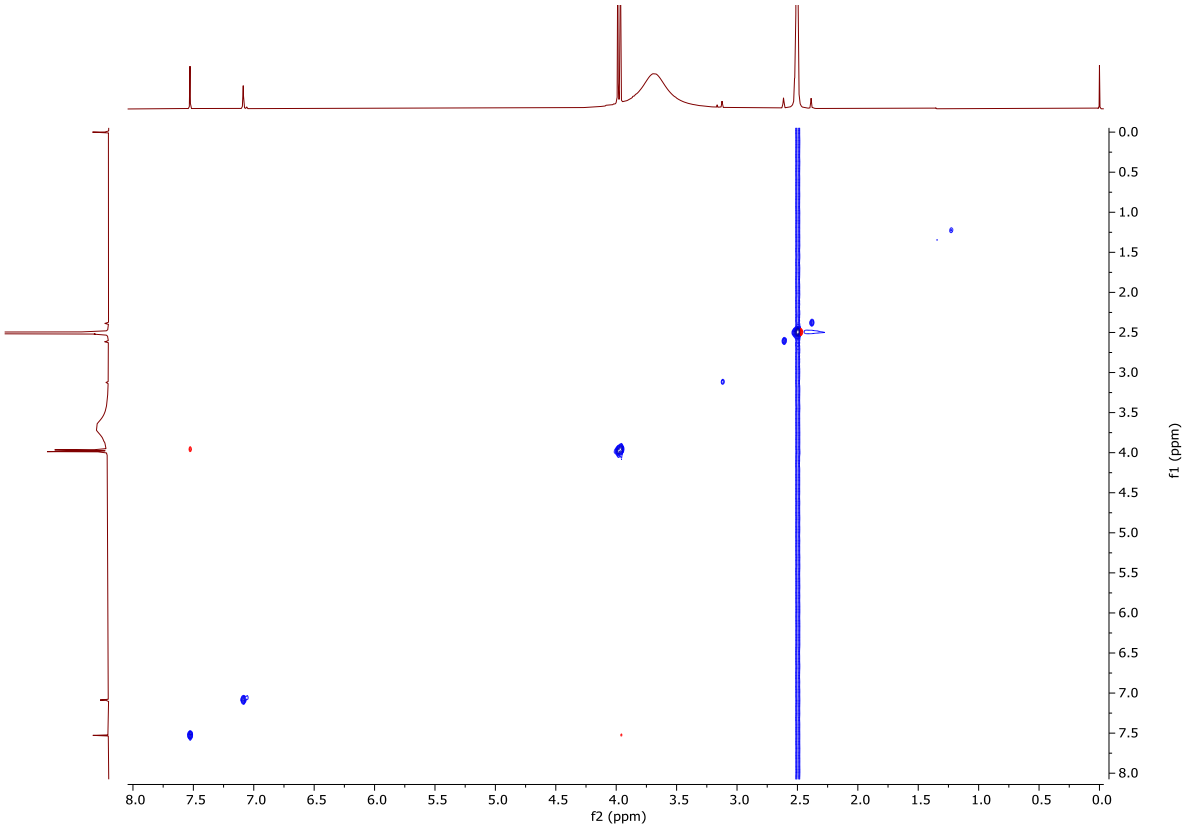


**Figure S8-4.** ROESY spectrum (DMSO-d6) of 3,4-di-*O*-methylellagic acid (**13**).

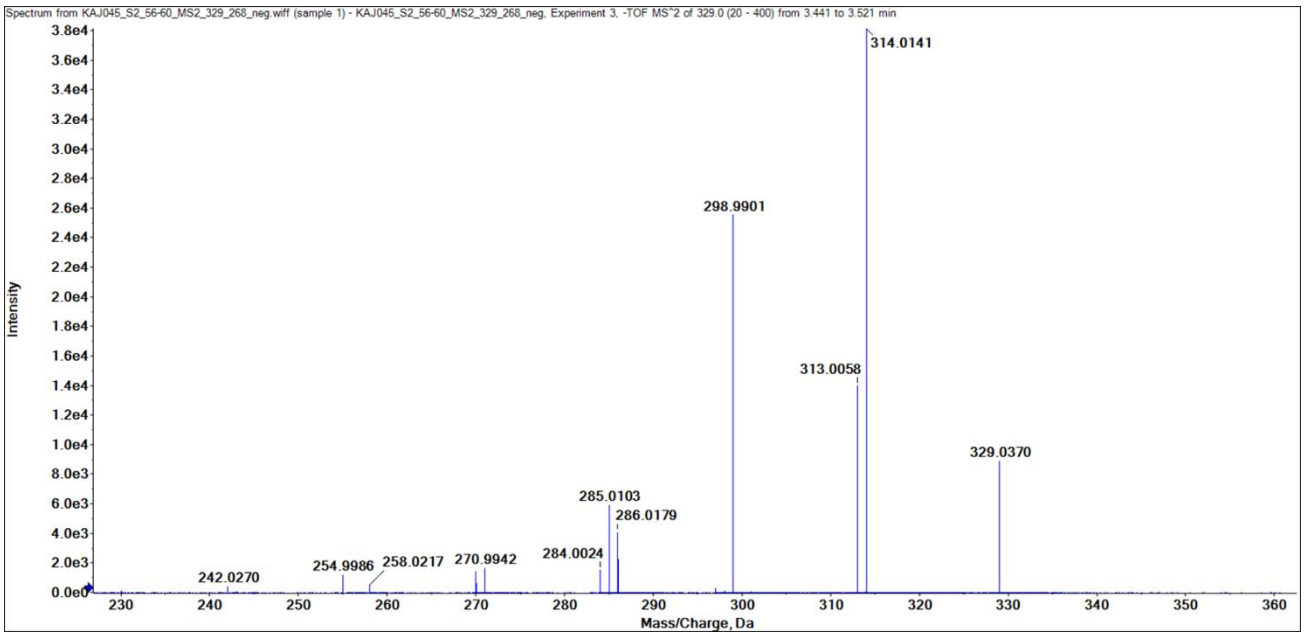


**Figure S8-5.** MS2 spectrum of 3,4-di-*O*-methylellagic acid (**13**) acquired with a QqTOF mass spectrometer in negative ion mode.

**Table S5.** NMR spectroscopic data (400 MHz, DMSO-*d6*) for 3,3′,4′-tri-*O*-methylellagic acid 4-sulfate (**15**).

| position | $\delta_C$, type | $\delta_H$ | NOESY | HMBC |
|---|---|---|---|---|
| 1 | 112.96, C | | | |
| 2 | 140.86, C | | | |
| 3 | 143.32, C | | | |
| 4 | 147.64, C | | | |
| 5 | 117.61, CH | 8.24, s | | 1, 2, 3, 4, 6, 7 |
| 6 | 111.52, C | | | |
| 7 | 158.31, C=O | | | |
| 1‘ | 114.13, C | | | |
| 2‘ | 140.89, C | | | |
| 3‘ | 141.34, C | | | |
| 4‘ | 154.37, C | | | |
| 5‘ | 107.50, CH | 7.66, s | 4‘-OMe | 1‘,2‘, 3‘, 4‘, 6‘, 7‘ |
| 6‘ | 112.83, C | | | |
| 7‘ | 158.46, C=O | | | |
| 3‘-OMe | 61.32, $CH_3$ | 4.06, s | | 2‘ |
| 4‘-OMe | 56.75, $CH_3$ | 4.02, s | 5‘ | 4‘ |
| 3-OMe | 61.47, $CH_3$ | 4.12, s | | 3 |

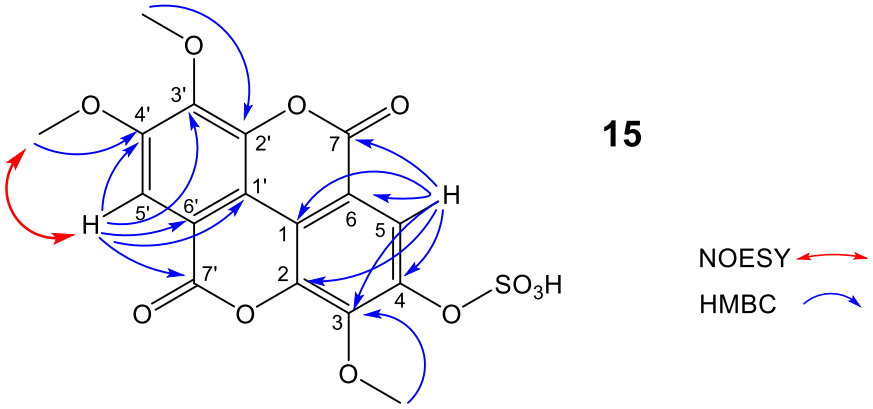

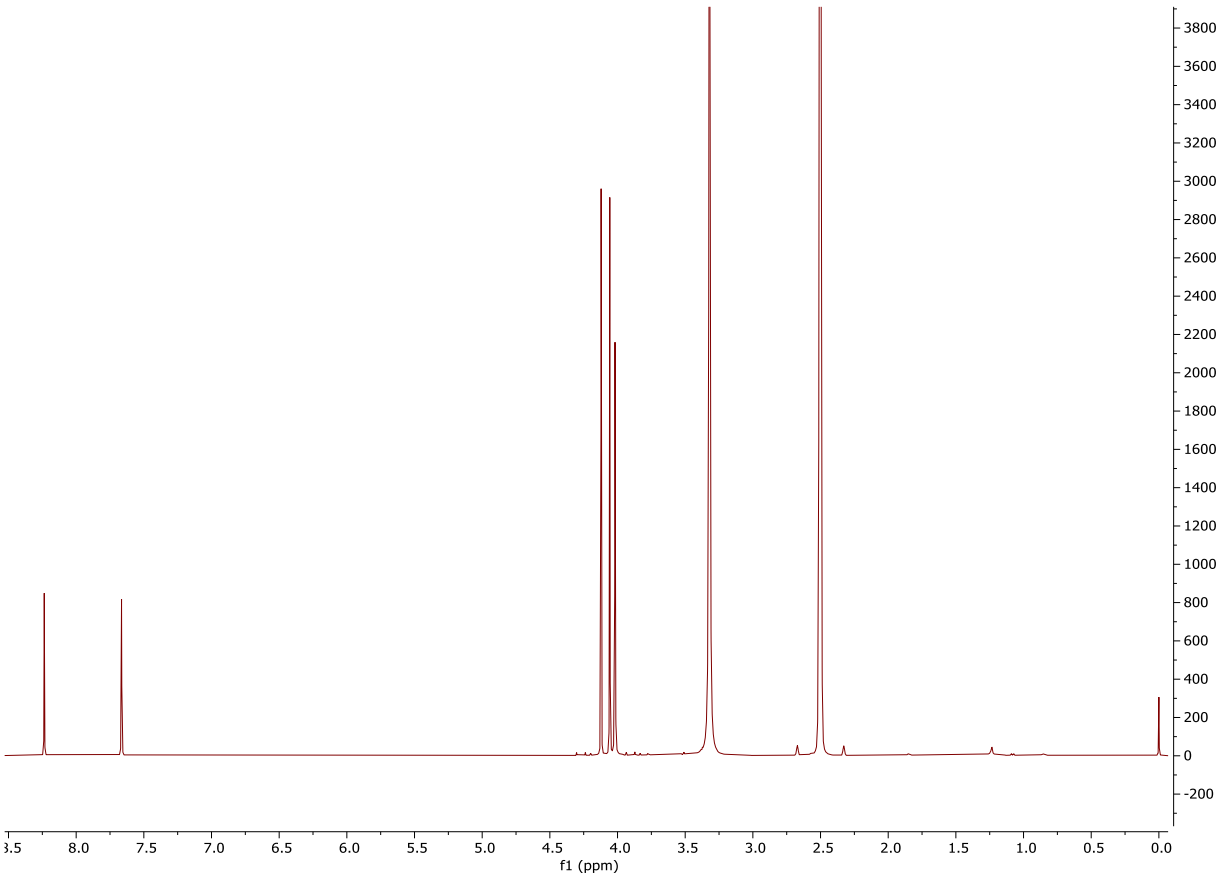


**Figure S9-1.** $^{1}$H NMR spectrum of 3,3′,4′-tri-*O*-methylellagic acid 4-sulfate (**15**).

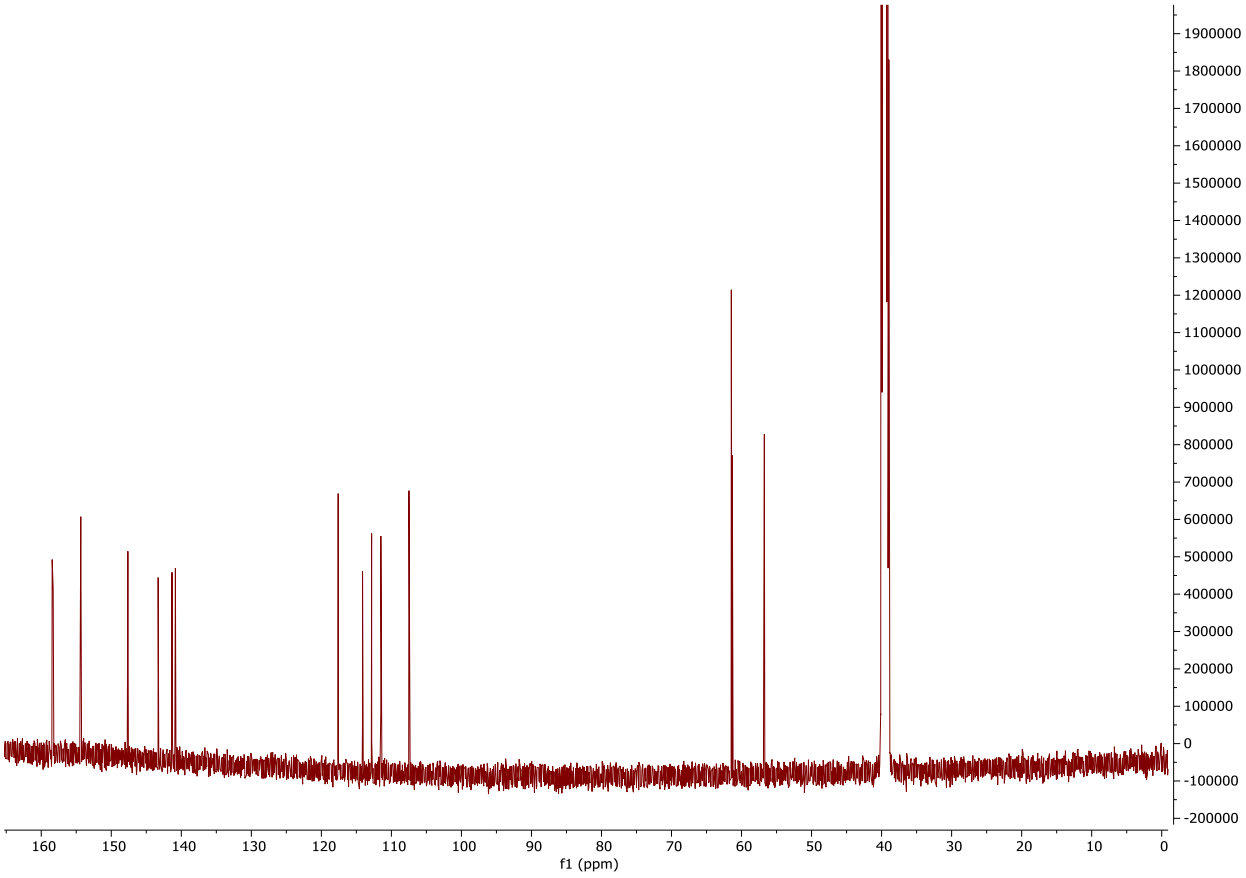


**Figure S9-2.** $^{13}$C NMR spectrum of 3,3′,4′-tri-*O*-methylellagic acid 4-sulfate (**15**).

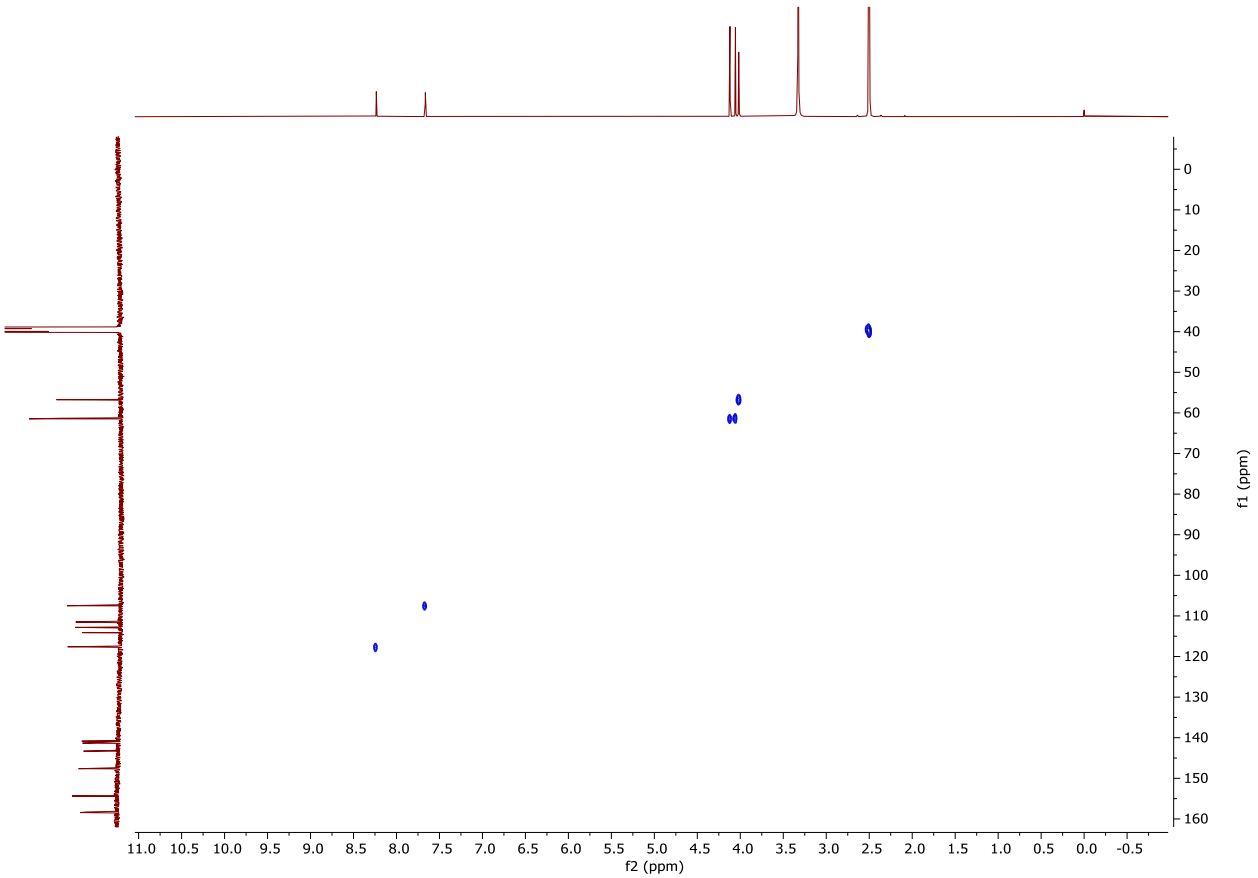


**Figure S9-3.** HSQC spectrum of 3,3′,4′-tri-*O*-methylellagic acid 4-sulfate (**15**).

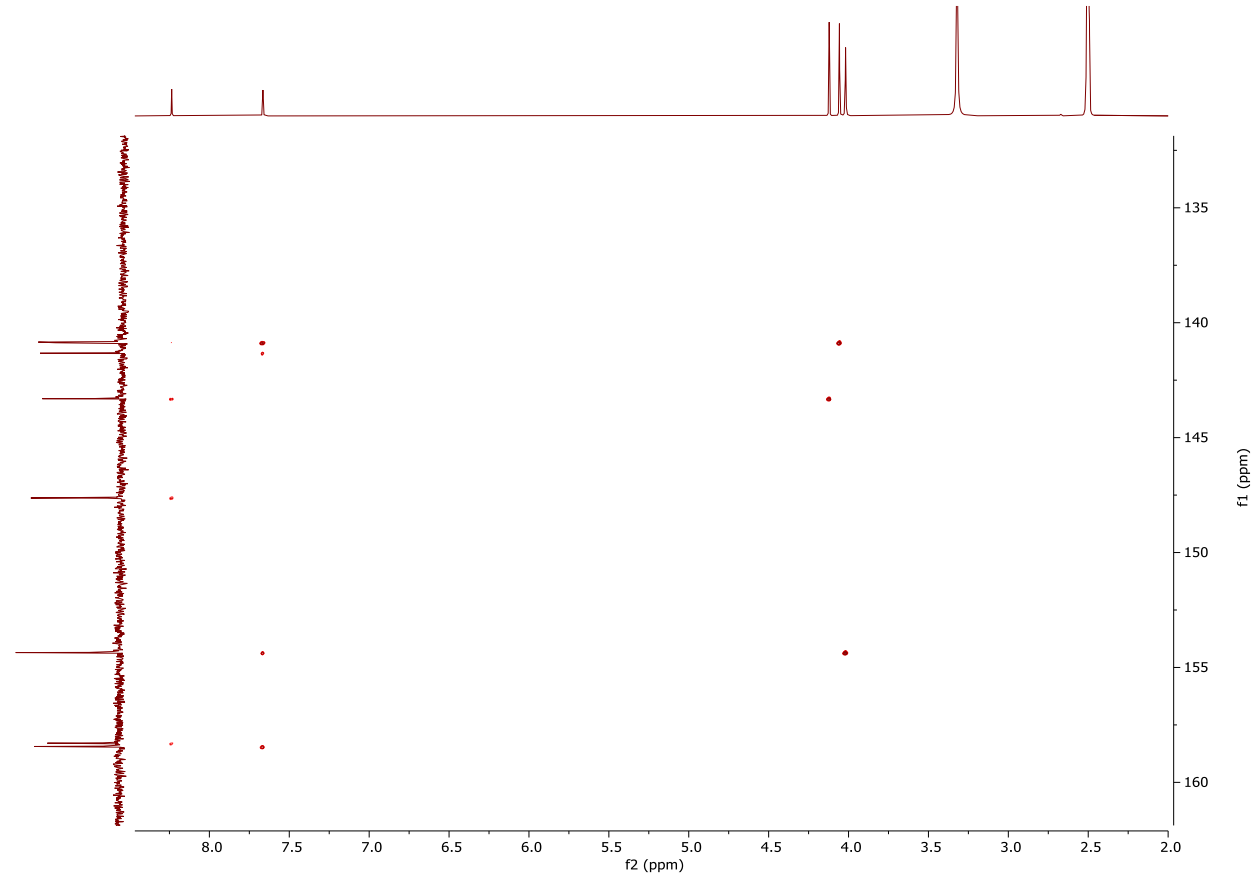


**Figure S9-4.** HMBC spectrum of 3,3′,4′-tri-*O*-methylellagic acid 4-sulfate (**15**).

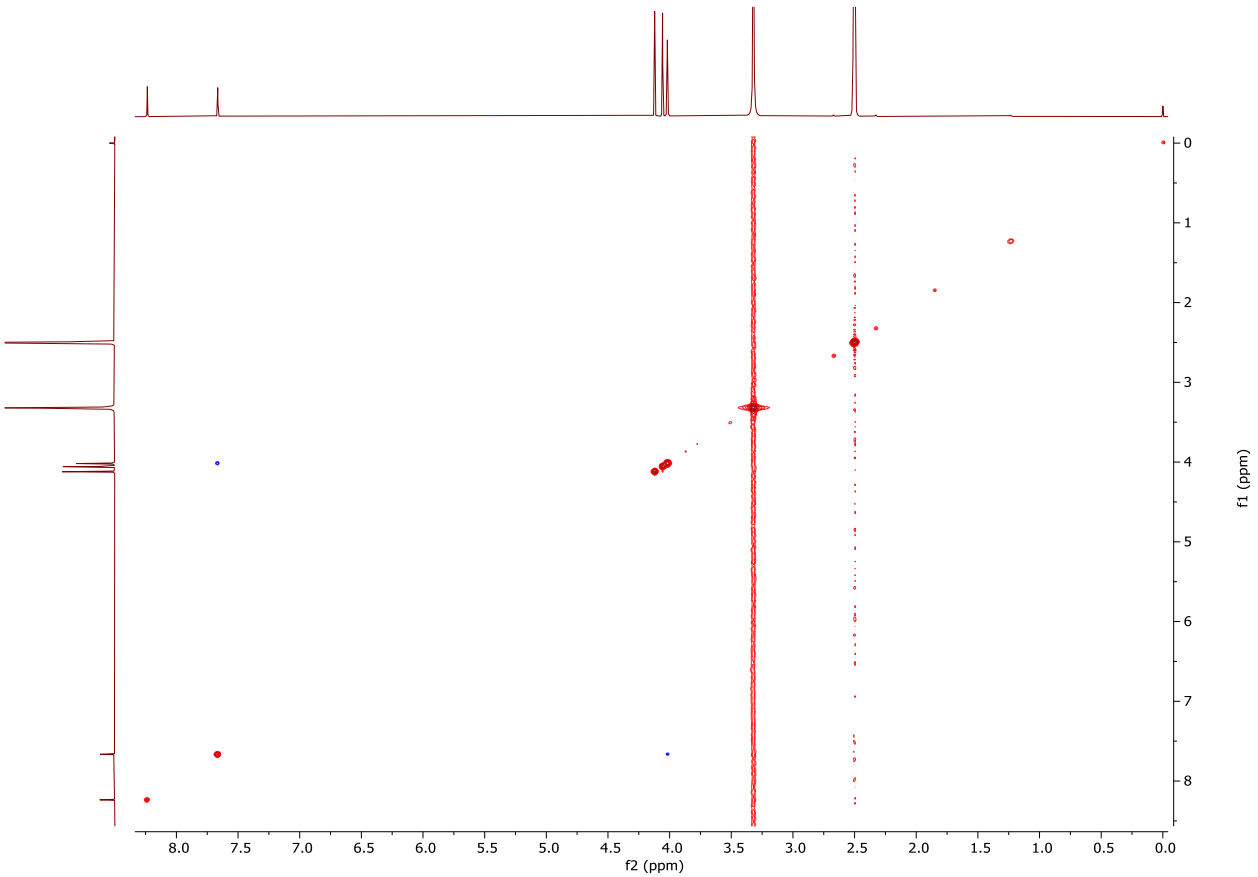


**Figure S9-5.** NOESY spectrum of 3,3′,4′-tri-*O*-methylellagic acid 4-sulfate (**15**).

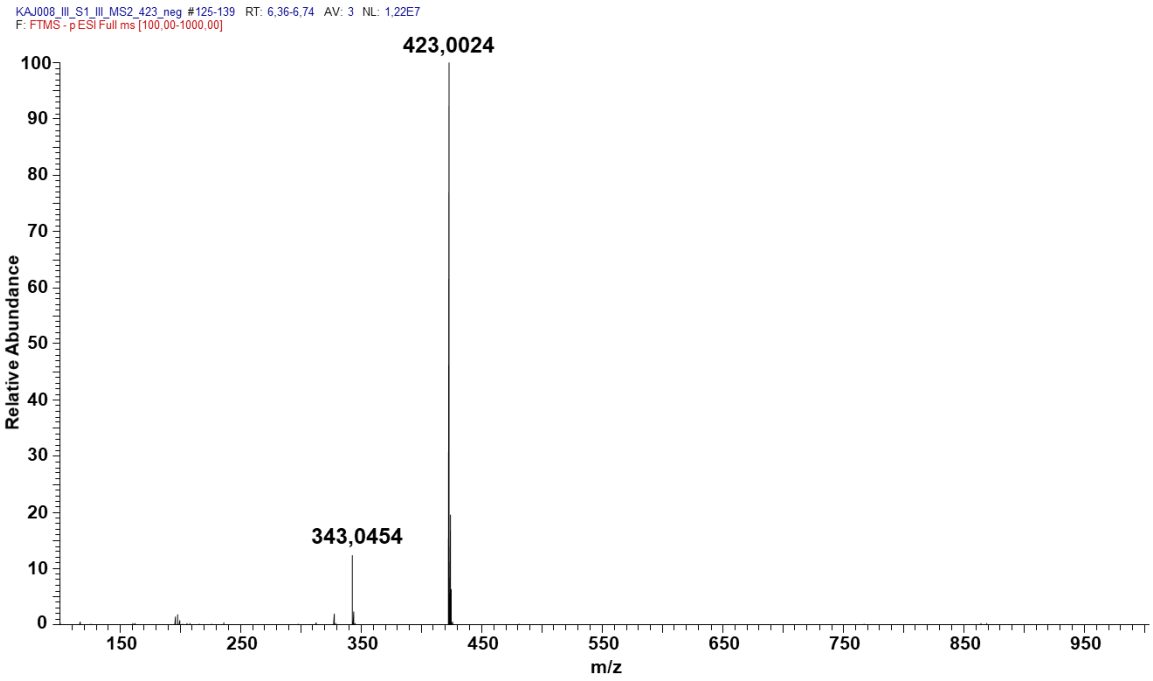


**Figure S9-6.** Full HRMS spectrum of 3,3′,4′-tri-*O*-methylellagic acid 4-sulfate (**15**) acquired with LIT-Orbitrap-MS in negative ion mode.

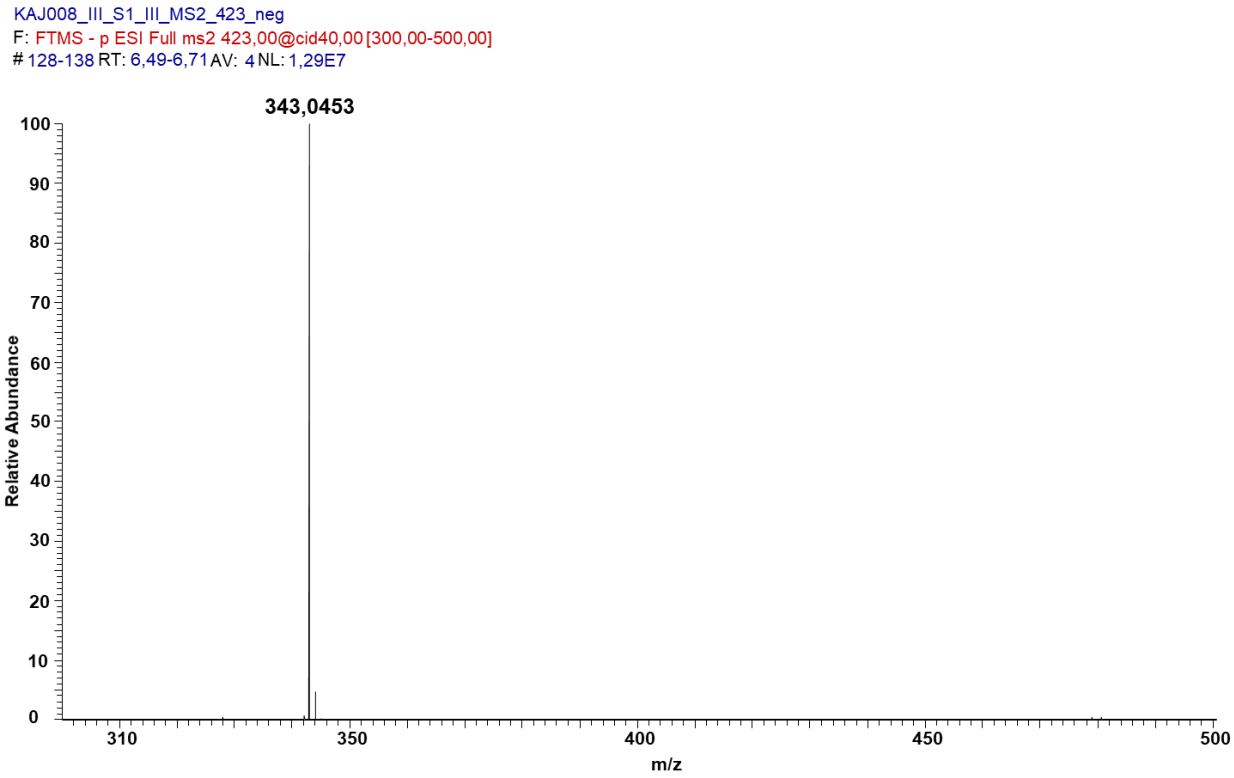


**Figure S9-7.** MS2 spectrum of 3,3′,4′-tri-*O*-methylellagic acid 4-sulfate (**15**) acquired with LIT-Orbitrap-MS in negative ion mode with CID activation (40% relative collision energy).

**Table S6.** NMR spectroscopic data (400 MHz, DMSO-*d6*) for 3,3′,4′-trimethylellagic acid (**16**).

| position | $\delta_C$ | $\delta_H$ (J in Hz) | NOESY | HMBC |
|---|---|---|---|---|
| 1 | 110.80, C | | | |
| 2 | 140.67, C | | | |
| 3 | 140.18, C | | | |
| 4 | 152.96, C | | | |
| 5 | 111.67, CH | 7.52, s | | 1, 3, 4, 6, 7 |
| 6 | 112.39, C | | | |
| 7 | 158.24, C=O | | | |
| 1′ | 111.74, C | | | |
| 2‘ | 141.37, C | | | |
| 3‘ | 140.85, C | | | |
| 4‘ | 153.62, C | | | |
| 5‘ | 107.33, CH | 7.61, s | 4‘-OMe | 1‘, 3‘ ,4‘, 6‘, 7‘ |
| 6‘ | 113.33, C | | | |
| 7‘ | 158.44, C=O | | | |
| 3‘-OMe | 61.19, $CH_3$ | 4.04, s | | 3‘ |
| 4‘-OMe | 56.60, $CH_3$ | 4.00, s | 5‘ | 4‘ |
| 3-OMe | 60.83, $CH_3$ | 4.06, s | | 3 |

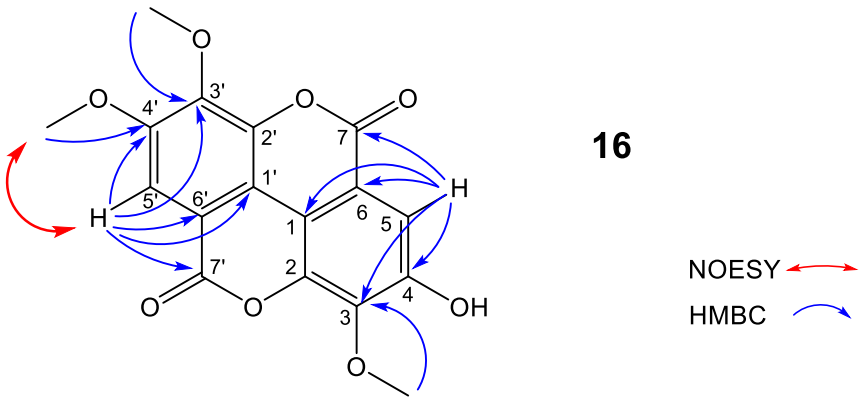

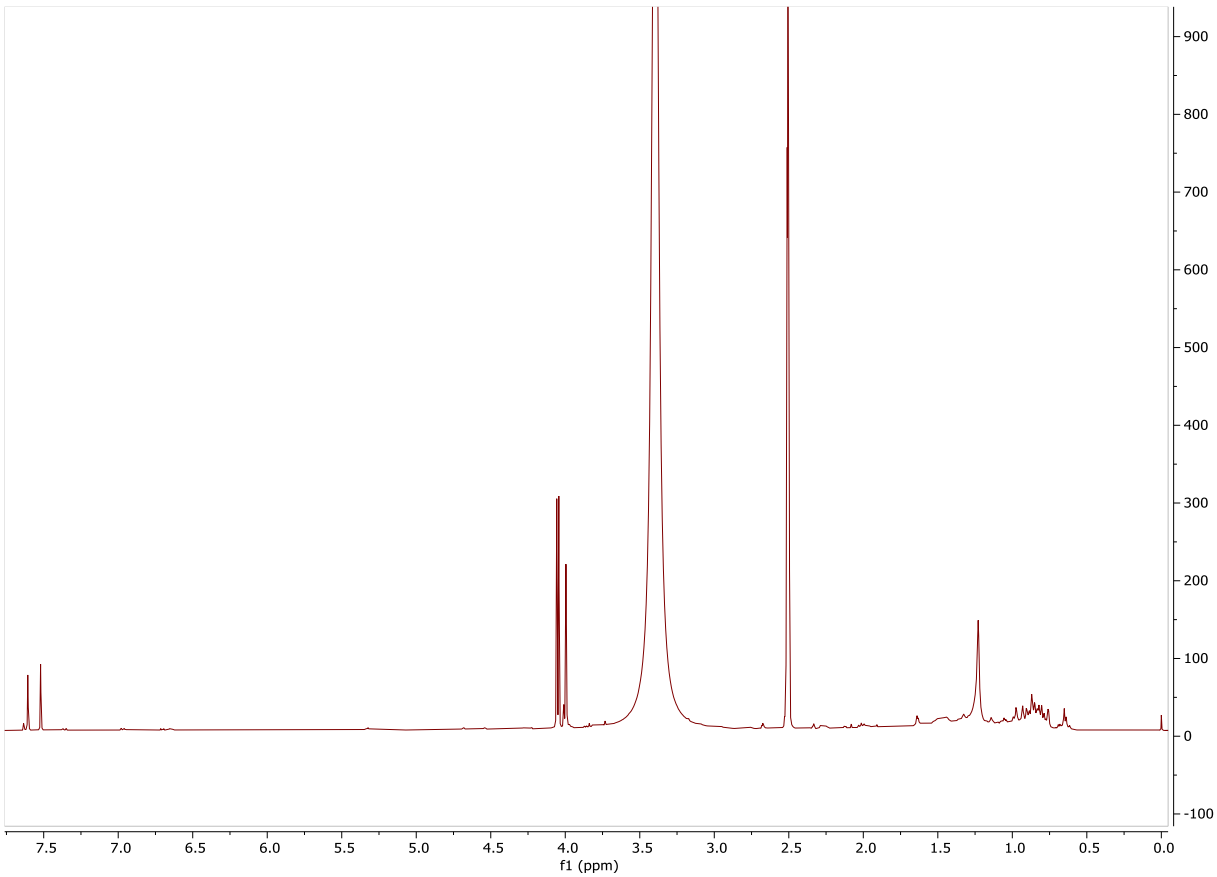


**Figure S10-1.** $^{1}$H NMR spectrum of 3,3′,4′-tri-*O*-methylellagic acid (**16**).

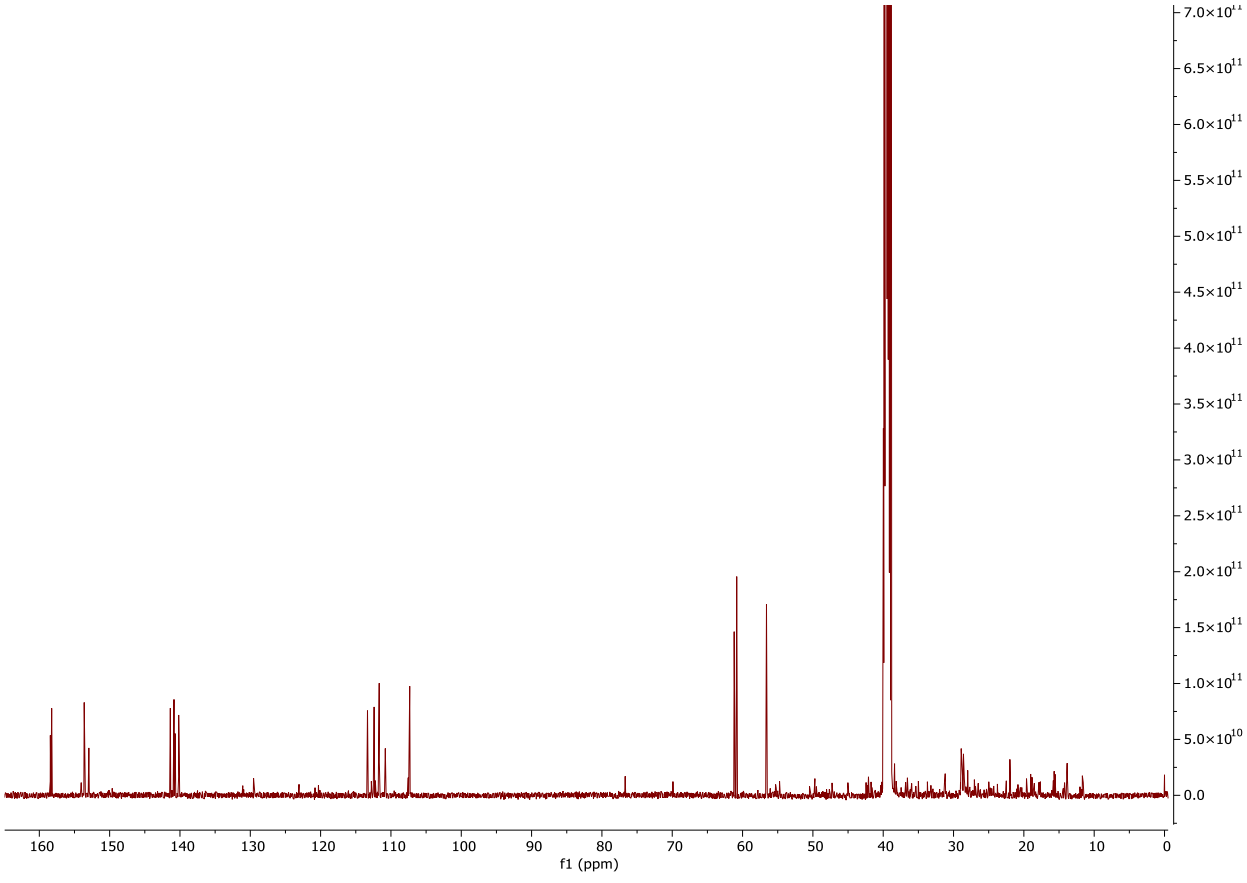


**Figure S10-2.** $^{13}$C NMR spectrum of 3,3′,4′-tri-*O*-methylellagic acid (**16**).

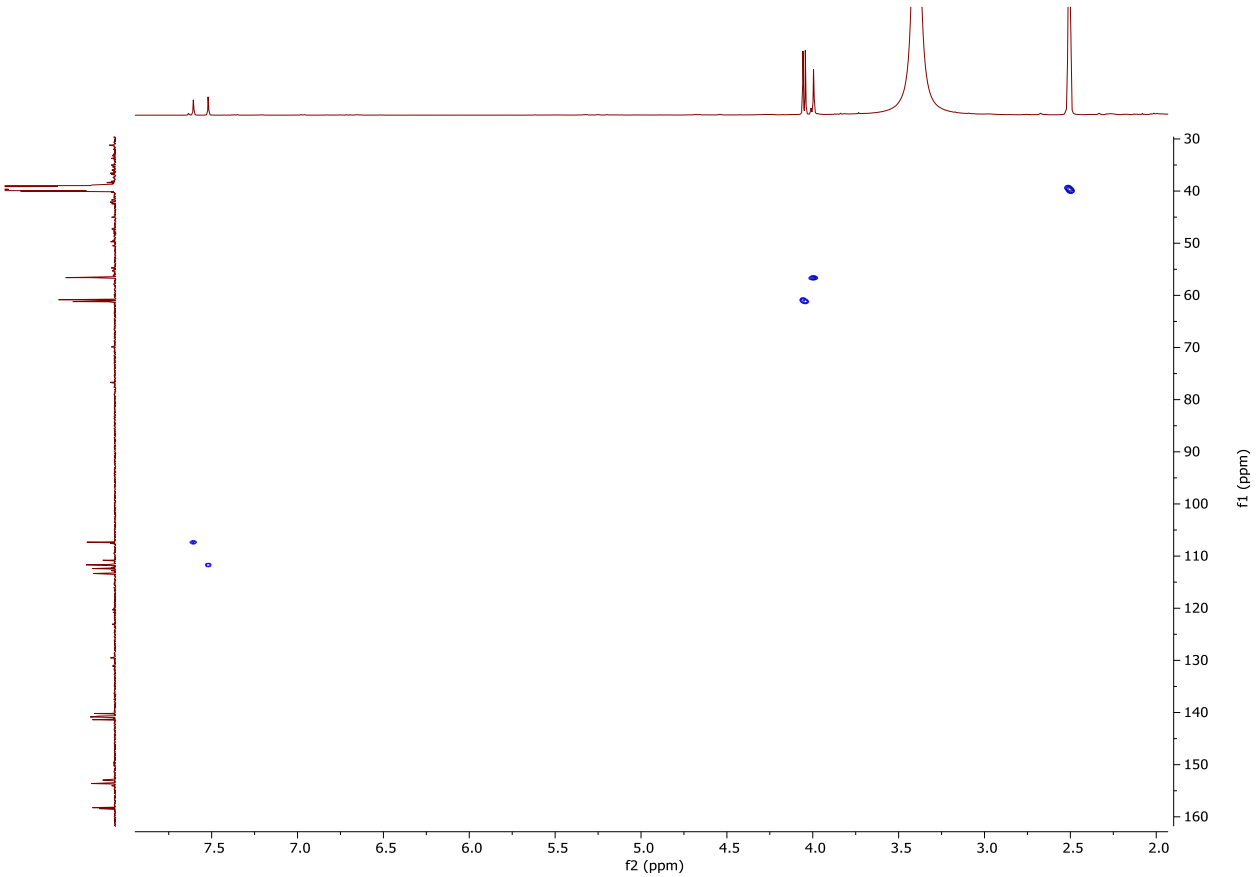


**Figure S10-3.** HSQC spectrum of 3,3′,4′-tri-*O*-methylellagic acid (**16**).

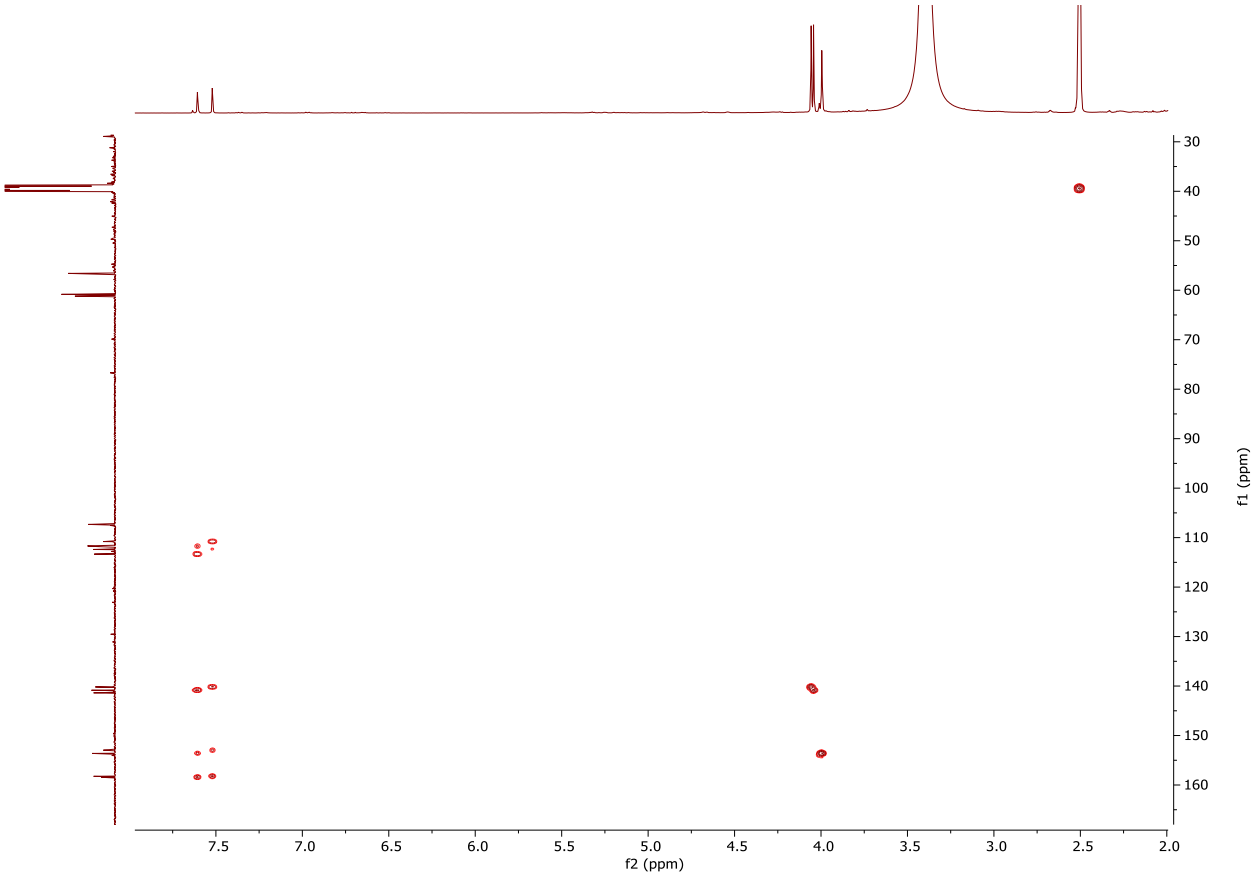


**Figure S10-4.** HMBC spectrum of 3,3′,4′-tri-*O*-methylellagic acid (**16**).

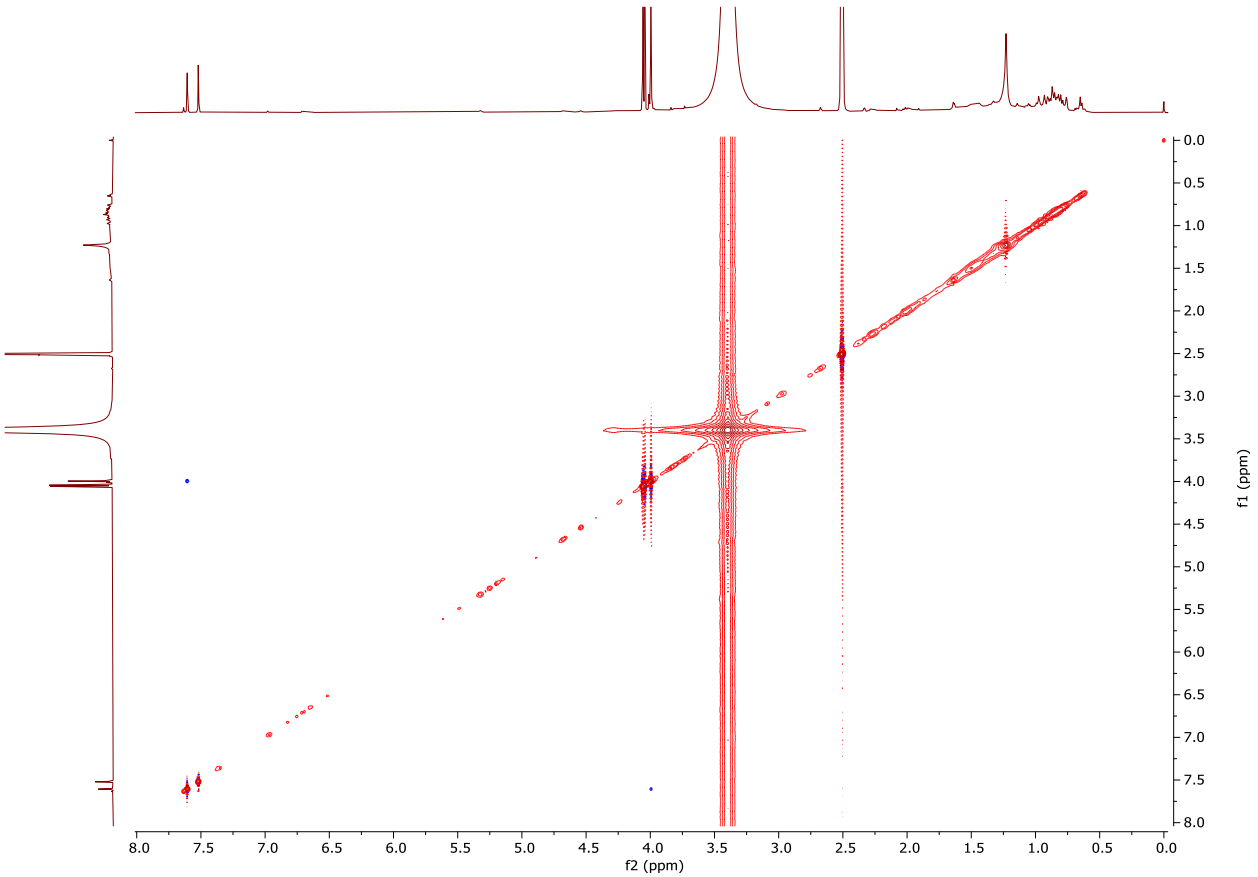


**Figure S10-5.** NOESY spectrum of 3,3′,4′-tri-*O*-methylellagic acid (**16**).

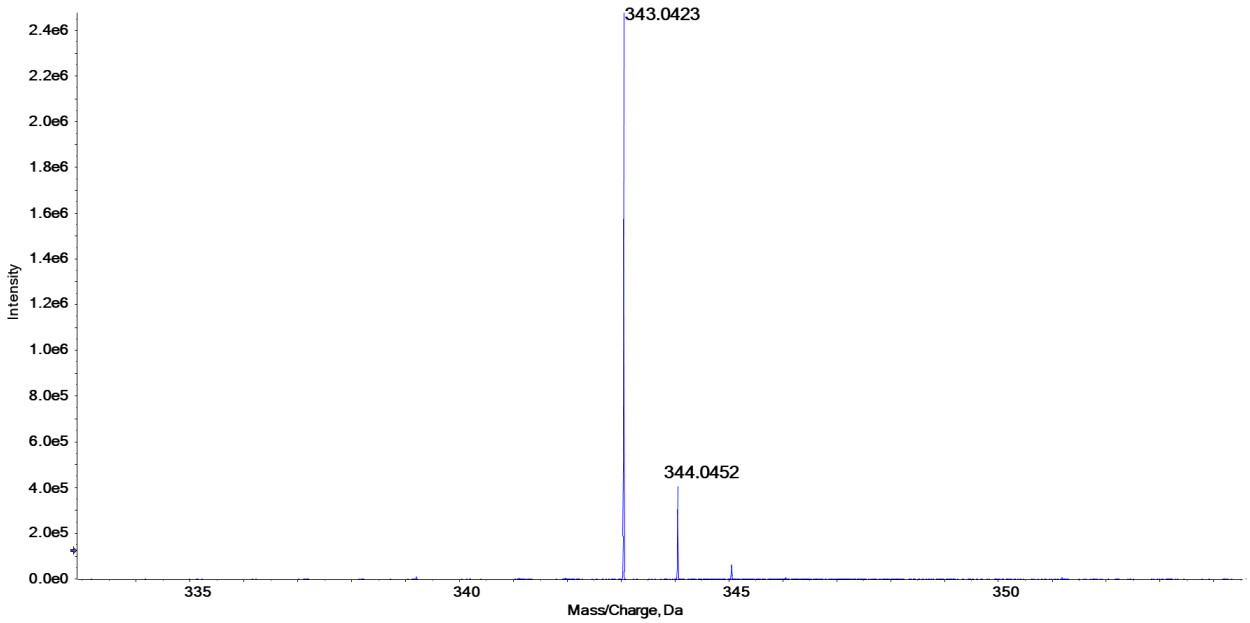


**Figure S10-6.** Negative HR-MS spectrum of 3,3′,4′-tri-*O*-methylellagic acid (**16**) acquired with a QqTOF mass spectrometer.

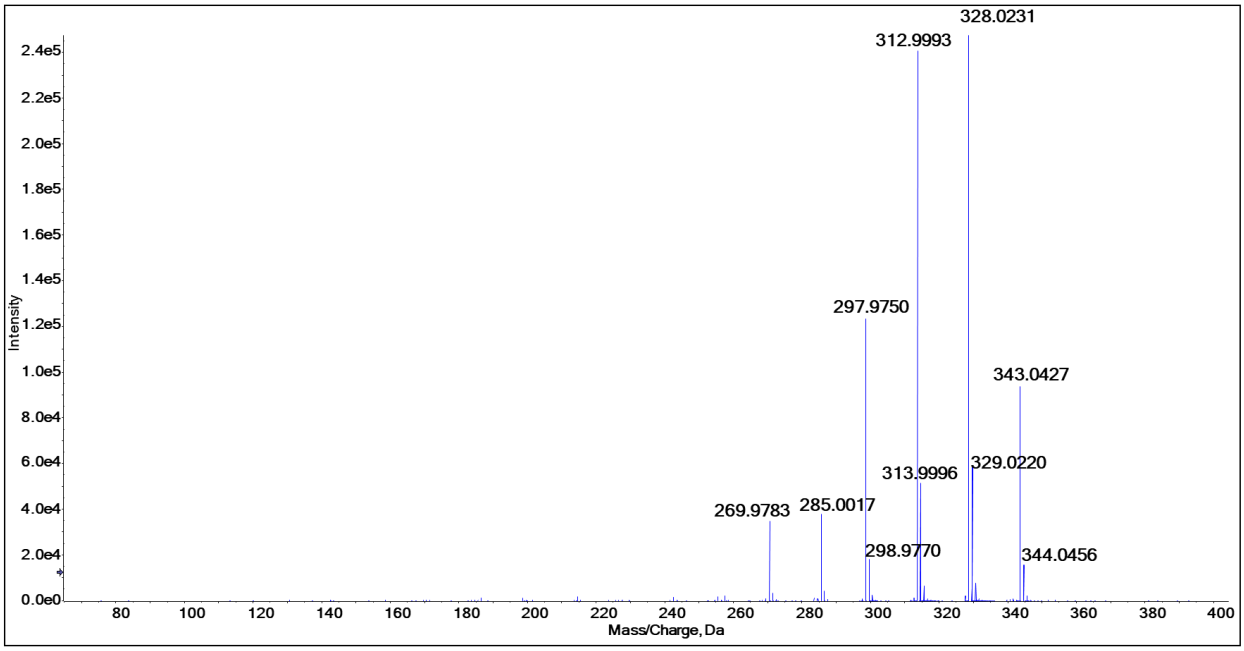


**Figure S10-7.** MS2 spectrum of 3,3′,4′-tri-*O*-methylellagic acid (**16**) acquired with a QqTOF mass spectrometer in negative mode.